Department of Chemical Engineering

Development of Carbon Nanotube Supported Pt NPs for Oxygen Reduction of Fuel Cells

Haohua Kuang

This thesis is presented for the Degree of

Master of Philosophy (Chemical Engineering)

of

Curtin University

September 2017

Declaration

To the best of my knowledge and belief this thesis contains no material previously published by any other person except where due acknowledgment has been made.

This thesis contains no material which has been accepted for the award of any other degree or diploma in any university.

Signature: …….

Date: ……...

Acknowledgements

I would also like to thank my supervisors Sanping JIANG and Chunzhu LI for their patience in what has been a longer than expected project.I would also like to thank Yi CHENG and Jin ZHANG for helping me togetsuitable necessaries and setting up the electrochemicalworkstation. Also, there are many thanks to Shuai HE for supporting this project and analysing the TEM data. I would like to thank all the staff at FETI for making my short time there a memorable and enjoyable experience.Last but not least,I am very fortunate that my wife, Emily, does not object to having poles and wires around and over the house and that there have been no complaints from neighbours.

Abstract

Carbon nanotubes (CNTs) have been widely investigated to develop efficient ORR catalysts and metals loading, which can dramatically improve their activity for ORR. Here for the first time we demonstrate that number of walls in pristine CNT supports has significant effects on the electrocatalytic activity of Pt nanoparticles (NPs) towards ORR in both alkaline and acidic conditions, with the electrocatalytic activity of Pt NPs showing distinctive volcano-type curves as a function of the number of walls. In this study, Pt NPs of a similar size were uniformly self-assembled on CNTs with different number of walls and outer diameters, which could be used as model catalysts. Characterization methods including Transmission electron microscopy(TEM), Brunauer-Emmett-Teller(BET), X-ray diffraction (XRD), thermogravimetric analysis (TGA) and electrochemical activities were applied in order to confirm the loading, particle size and distribution of platinum nanoparticle onto various types to carbon nanotubes. The electrochemicalperformance of Pt/CNTs was identified through electron transfer number and Tafel slope through LSV analysis both in alkaline and acidic solutions. Double-walled CNTs (DWCNTs) composed of 2-3 walls exhibit better activity for ORR, compared with typical single-walled CNTs (SWCNTs) and multi-walled CNTs (MWCNTs). The findings explored a direction for developing high active and stable electrocatalysts for energy conversion technology.

Key words: Carbon nanotubes, Oxygen reduction reaction, Functionalization, Pt

Contents

List of Figures

List of Tables

1 Introduction

1.1 Oxygen Reduction Reaction

1.1.1 General Description

Over reliance on traditional energy resources, such as coal, natural gas, oil and firewood, leads to detrimental environmental impact and is not sustainable[1]. Using fossil fuels have some side effects, including generating greenhouse gases and sulphur dioxide (SO_2) and possessing low efficiency. Greenhouse gas like carbon dioxide (CO_2) is warming up the globe, glaciers would then melt at a faster speed and the sea level would rise up as a consequence. SO_2 results in acid rain, eroding buildings and outside machines. Meanwhile, this process is rather low efficient and cannot meet the rising global energy demand.So, relying on traditional energy resources will poses serious challenges to human health, energy security, and environmental protection.

In order to solve this problem, fuel cell technology has drawn significant attention from researchers and companies because of no pollution, high energy conversion efficiency and potential large-scale applications. Fuel cell technology is believed to be the most promising solution for its sustainable and clean power[2]. Water is the only by product of this system, which directly generates electricity by electrochemically reducing oxygen and oxidizing fuel into water. Meanwhile, this energy conversion technology possesses rather high efficiency and it can be applied in various areas, like automobiles and factories.

Fuel cells are separated into different types and in this research they are mentioned as following kinds: polymer electrolyte membrane fuel cells (PEMFC), direct methanol fuel cells, alkaline fuel cells, phosphoric acid fuel cells, molten carbonate fuel cells, solid oxide fuel cells and reversible fuel cells. Among them, the hydrogen/air PEMFC is believed to be the most available fuel cell for automotive propulsion, which is also the main target of my research.

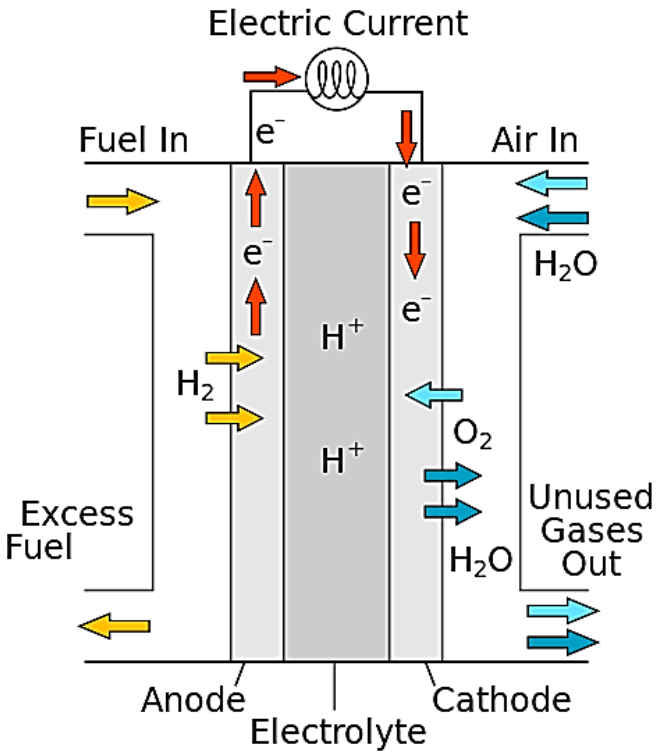

Fig 1Scheme of a proton-conducting fuel cell [6]

As shown in the scheme of a proton conducting fuel cell in figure 1, it consists of two anodes (anode and cathode), a membrane, an electrolyte and catalysts. Anode is the place where H_2 inputs and cathode is the place where oxygen inputs. Membrane is used to exchange proton and prohibit the gas diffusion of hydrogen (H_2) and oxygen (O_2). Catalysts are sprayed or painted onto a carbon paper and they are catalysing H_2 and O_2 As for catalysts, platinum (Pt) based catalysts are mainly mentioned in this paper because the main purpose of this paper is researching the effect of the number of wall of carbon nanotubes on the electrochemical performance of Pt. Pt based catalysts include Pt and Pt alloys.

But, the cost and performance aims for this application are still challenging. It is well acknowledged that the conversion efficiency into mechanical energy is necessary to reach an acceptable fuel cost for per kilometre as the cost of producing clean H_2 from water can hardly be negligible. Also, driving range has a strong relationship with the efficiency. Since the energy density of compressed H_2 is rather low, it is still challenging to get enough ft. for a driving range longer than 400 km[3]. But, this can somehow be moderated by the more adorable efficiency of the PEFC compared to the relevant efficiency of a traditional power train/ICE**.** PEFC cars using condensed H_2 have reached a driving range of 500 km. For the purpose of urban use,

battery cars without any fuel plug-in possessing 150 km driving ranges somehow can be applied. But there are still many limitations related to the battery cost and weight and charging time. In this thesis, we present the recent fundamentals and advances concerning to the fields of ORR, with a focus on the electrochemistry and materials chemistry of ORR. The catalytic mechanism and battery electrochemistry of oxygen reduction reactions (ORR) both in acidic and alkaline solution are discussed on the basis of organic and aqueous electrolytes.

As for the catalytic mechanism, several common ORR processes and their relevant thermodynamic electrode potentials at different standard conditions are listed in the following parts. The mechanism of the electrochemical O_2 reduction reaction is relatively complexed and contains tons of intermediates, which has a strong relationship with the conditions of the electrode material, electrolyte and catalysts. The mechanism of various catalysts would also be listed.

But, there are two main pathways included, that is, the 2-electron reduction pathway and the direct 4-electron reduction pathway[4]. The former one is from oxygen (O_2) to hydrogen peroxide (H_2O_2) and the later one is from O_2 to H_2O. Admittedly, in non-aqueous aprotic solvents and/or in alkaline solutions, one special pathway, namely, the pathway from O_2 to superoxide exists.

It is well known that the mechanism in acidic and alkaline is different. Specifically, there are five elemental steps involved in acidic condition, that is, the dissociation of O_2, two hydrogenation steps of both O and OH.

In acidic aqueous solution, there are three steps involved:

$O_2 + 4H^+ + 4e = H_2O$ 1.229V

$O_2 + 2H^+ + 2e = H_2O_2$ 0.70V

$H_2O_2 + 2H^+ + 2e = 2H_2O$ 1.76V

In alkaline aqueous solution, there are also three steps involved:

$O_2 + H_2O + 4e = 4OH$ 0.401V

$O_2 + H_2O + 2e = HO_2^- + OH$ -0.065V

$HO_2^- + H_2O + 2e = 3OH^-$ 0.867V

In non-aqueous aprotic solvents, there are only two relevant steps:

$O_2 + e = O_2^-$ a

$O_2^- + e = O_2^{2-}$ b

a, b: The thermodynamic potentials for the 1-electron reduction reaction to form a superoxide, as well as the values are not fixed because their further reductions into O_2^{2-} are mainly dependent on the solvent used.

1.2 Catalysts

As mentioned above, the proton exchange membrane (PEM) is consisted of two anodes, that is, cathode and anode. Compared to the hydrogen oxidation reaction in the anode, ORR in the cathode is six orders of magnitude slower because of its large onset over potential and sluggish kinetics. One another reason for this is that there are only two electrons involved in hydrogen oxidation reaction while there are four electrons in ORR. At the moment, Pt is the most commonly used catalyst, which is also the most cost component of the IC vehicles. So, in order to speed up the ORR kinetics to reach a practical point, proper catalysts with high catalytic activity and low expense should be investigated[5].

Therefore, many researches have been conducted in order to manufacture novel ORR catalysts byfollowing methods: increasing the mass activity by alloying the precious metal [6-9] with another metal and eliminating the existence of Pt by generating non-precious metal catalysts [10-13], which can be rather competitive.

1.2.1 Platinum

The state-of-the-art ORR catalysts are Pt and Pt based bimetallic or trimetallic electro-catalysts. It is clear that Pt is the only element which can meet the requirements while avoiding slow reaction kinetics, proton exchange membrane (PEM) system degradation caused byH_2O_2 formation and catalyst degradation related to metal leaching.

Using the Density functional theory (DFT) calculations[14], it is easy to get that the binding energy is relevant to catalytic efficiency. In specific, in order to gain high catalytic efficiency, the oxygen species should desorption from the surface of the catalyst. Or else, the catalyst would be poisoned by these species. Meanwhile, these species should also have strong adsorption affinity onto the surface of catalyst, so that the reaction would take place. Based on the two theoretical calculations mentioned before and experimental data, “volcano plots,” can be used getting the optimal ΔEO.

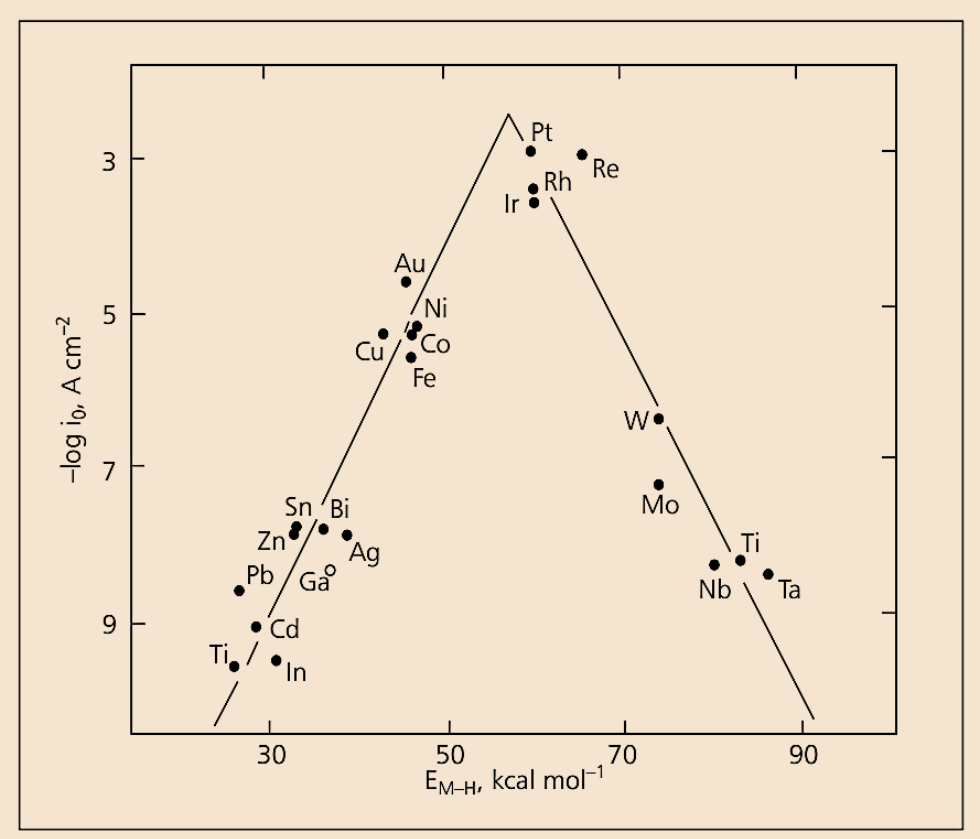

Fig 2 the logarithm of exchange current densities (logi0) for cathodic hydrogen evolution vs. the bonding adsorption strength of intermediate metal-hydrogen bond formed during the reaction itself[14].

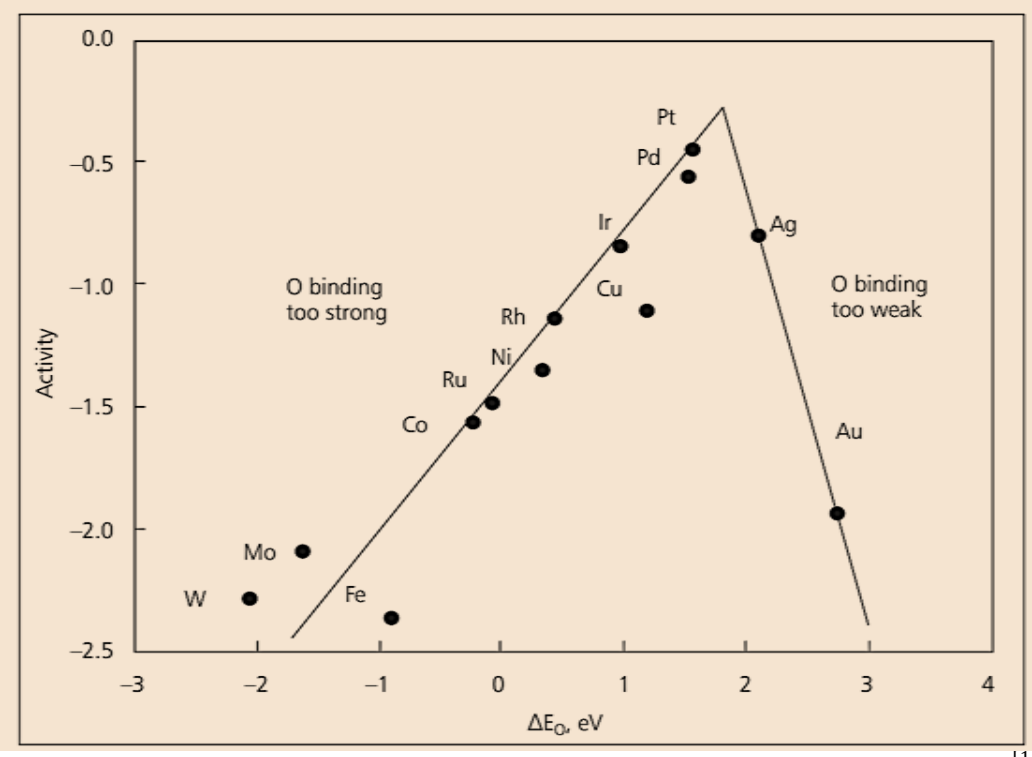

Fig 3 Trends in oxygen reduction activity plotted as a function of the oxygen binding energy[14].

Among these catalysts, Pt catalysts are located in the best position. This is the main reason for the wide utilization of Pt as catalyst. In this research, PtNano particle is the main part of the catalyst. Since the loading, distribution and nanoparticle size of Pt can have a significant effect on the catalytic efficiency; these parameters will be investigated by various methods.

Nevertheless, Pt does not takethe theoretical best position. So, while designing an ORR catalyst, it can be improved without any question. One solution to adjust oxygen intermediates' adsorption energies is adjusting the catalyst conductive band, or d-band centre. Another solution for shifting the catalyst electronics is tuning the main surface facets. There is a specific surface energy for each type of crystal plane.Besides, the activity of ORR would be enhanced more by applying a Pd_3Co nanoparticle core or Pt monolayer on a Pd results in a strain on this facet. In the following paper, Pt based catalysts will be introduced.

1.2.2 Platinum alloys

Pt alloys possess two obvious benefits compared to pure Pt catalysts. The first one is that those two metalinteractions tend to modify the electronic properties, resulting in higher ORR activity. Another one is that incorporated metal results in a decrease of the loading of Pt while catalytic activity maintained. This main reason for this phenomenonis that particle core is prohibited to leave the active site of Pt by alloying metal. There are some materials listed below that have embraced those benefits mentioned above in order to fabricate advanced catalysts.

1.2.2.1 Platinum-noble metal alloys

Given the fact that noble metals are stable in harsh condition of oxidation and acidic condition, it is beneficial to use them for ORR. Because of Ostwald ripening, they are excellent options as the addition of Pt catalysts which do not possess acceptable stability in PEMFCs.

Zhang et al. have produced a nano dendritic Ir@Pt catalyst through a one-pot synthesis solution[14]. Ir nano dendrites were prepared from the reduction of hexachloroiridic acid hexahydrate by sodium borohydride with the existence of CTAC at 60^oC for five hours. Through this method, Pt is homogeneous dispersed onto the surface of Ir with the molar ration of 0.5, which was confirmed by TEM analysis. Electrochemical surface area (ECSA) would be enhanced by the nature of these nano dendritic particles. Admittedly, the interaction between the Pt shell and

the iridium core can enhance the impressive ORR activity. The CV curve from 0 to 0.64V showed the improved catalytic performance. This is proposed to be attributed to the better dispersion of Pt and the interior interaction between Pt and Ir as well as the private morphology of Ir@Pt. This research has significance of proposing active bifunctional electrocatalysts.

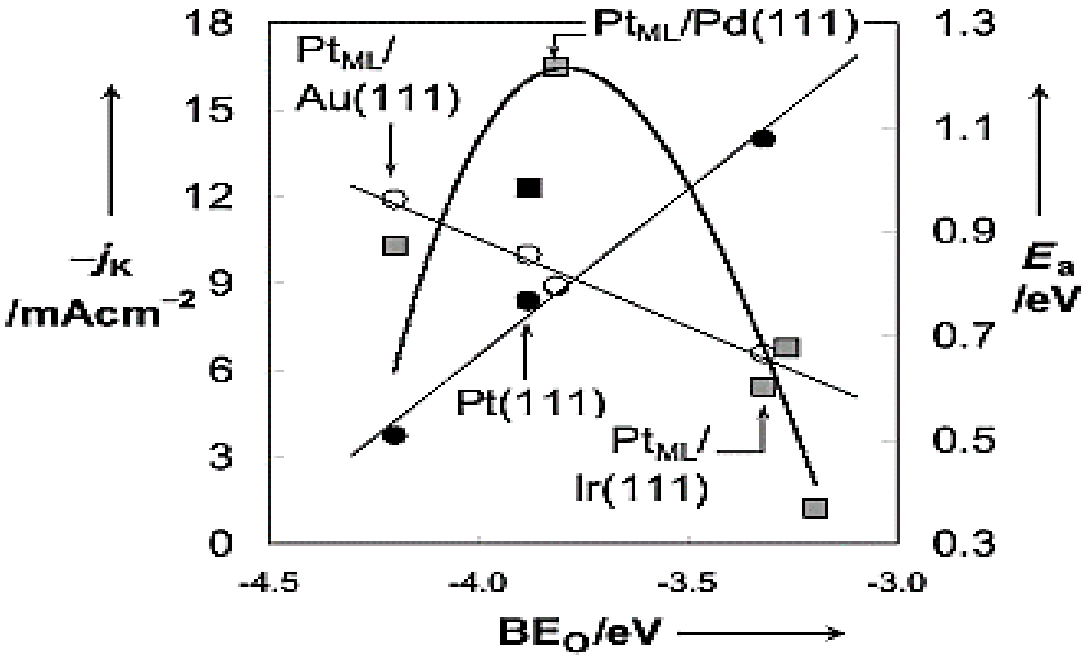

Fig 4 the oxygen reduction reaction (ORR) on Pt monolayers supported on various transition metals exhibits volcano-type behaviour[15]

Yeo et al. prepared Pt/Au nano dendrites by utilizing gold seed[15]. The background information for this process is that the hollow silica can provide an ideal place for consist growth of crystals. Meanwhile, the morphology of nanocrystals is also controllable. Most importantly, the silica shell is removable so that the inside crystals can be leaved. In this research, porous silica was applied with inner diameter of about 28nm. Pt nanoparticles were synthesised from the reduction of Na_2PtCl_4. HRTEM images and TEM analysis showed that Pt based Au nano dendrites were successfully prepared. Through ORR polarization curves in $HClO_4$ solution, spherical Pt/Au showed better catalytic performance when compared to that of Lf-PtND and commercial Pt blank. So, this research can provide an opportunity for novel preparation of hybrid nanocrystals. The electrocatalytic performance is expected to be enhanced in this way.

Fig 5 Synthesis of Pt nano-dendrite employs Au-seed-mediated growth inside hollow silica nanospheres[16]

Karan et al. produced a novel type of electrocatalyst, that is, Pt@IrPd. In this research, metal chlorides were reduced to synthesis samples with various molar ratios of Ir to Re[16]. Certain amount of metals was mixed with carbon before sonicated for half hour. Then, the mixture was dried and heat treated at four hundred centigrade. The reduced solid was tested by TEM and XAS as well as RDE. According to CV test, the half wave potential remained unchanged after 3000cycles. In other words, the stability of synthesised catalysts is adorable. This research is beneficial for the following reasons: Pt content can be decreased to be only one monolayer. Pt can be made full use because all atoms are participating in the reaction and there are more active sites compared to conventional catalysts. Tuneable activity and stability are enhanced by modifying the structure and electronic properties of Pt.

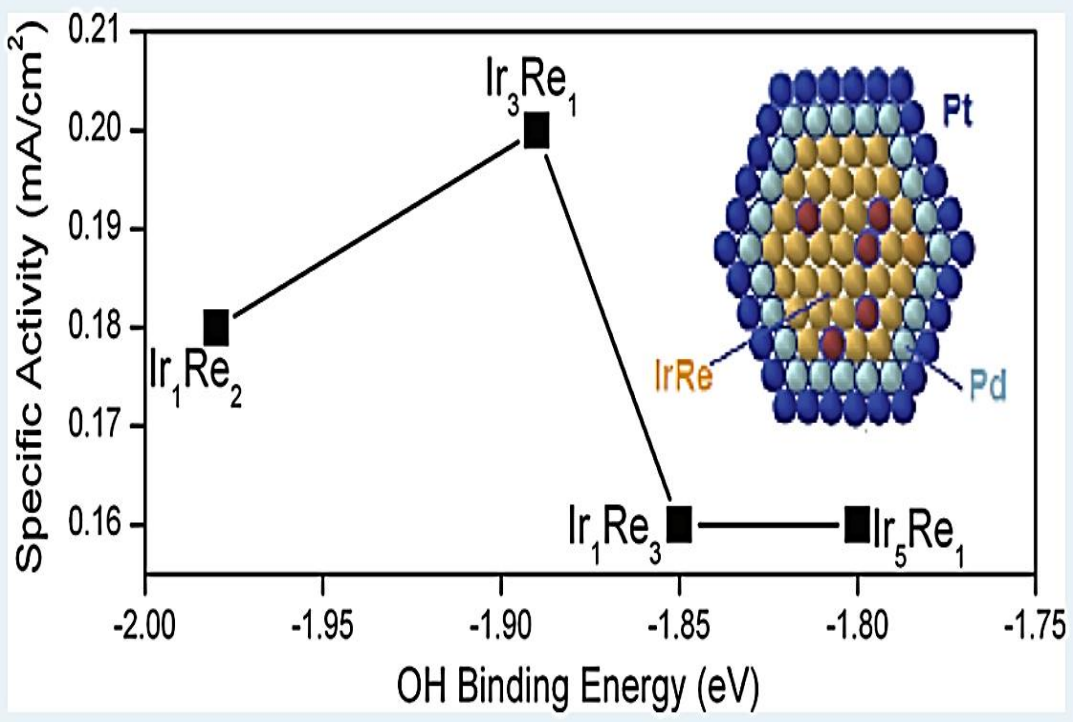

Fig 6 catalysts showed specific electro catalytic activity for ORR comparable to that of platinum[17].

Shao et al. prepared Pt monolayer supported onto the surface of Au. It showed better catalytic activity than Pt monolayer supported onto the surface of Pd and pure Pt. The pheromone was calculated and explained by density functional theory. The improved catalytic activity is believed to be contributed to the compressive strain in the surface of nanoparticles. Meanwhile, this paper mentioned that, conventionally, in order to decrease the amount of Pt content, core shell structure or adding replaceable materials are mainly applied[17].

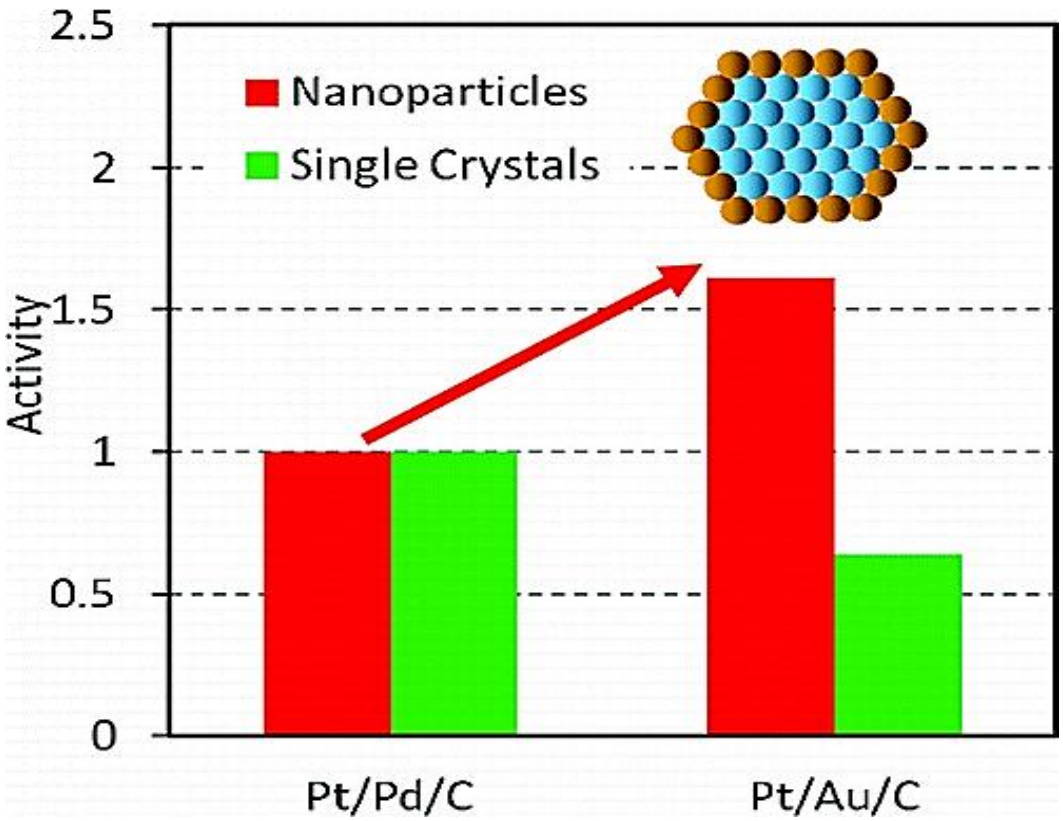

Fig 7the increase in oxygen binding energy was previously proposed to account for the lower oxygen reduction activity of a Pt monolayer supported on Au (111) single crystal than that on Pd (111) and pure Pt (111) surfaces[18].

Alia et al. have prepared three types of catalysts, that is, Pt coated palladium nanotubes, Pt nanotubes, and palladium nanotubes. Synthesised samples were characterized by SEM and TEM analysis. The result showed that nanotubes were doped with nanoparticles. According to area activity test, the performance of Pt/Pd nanotubes was far better than that of commercial Pt/C. This is believed to be contributed to the enhanced stability and morphology of Pt. The result is remarkable for further application[18].

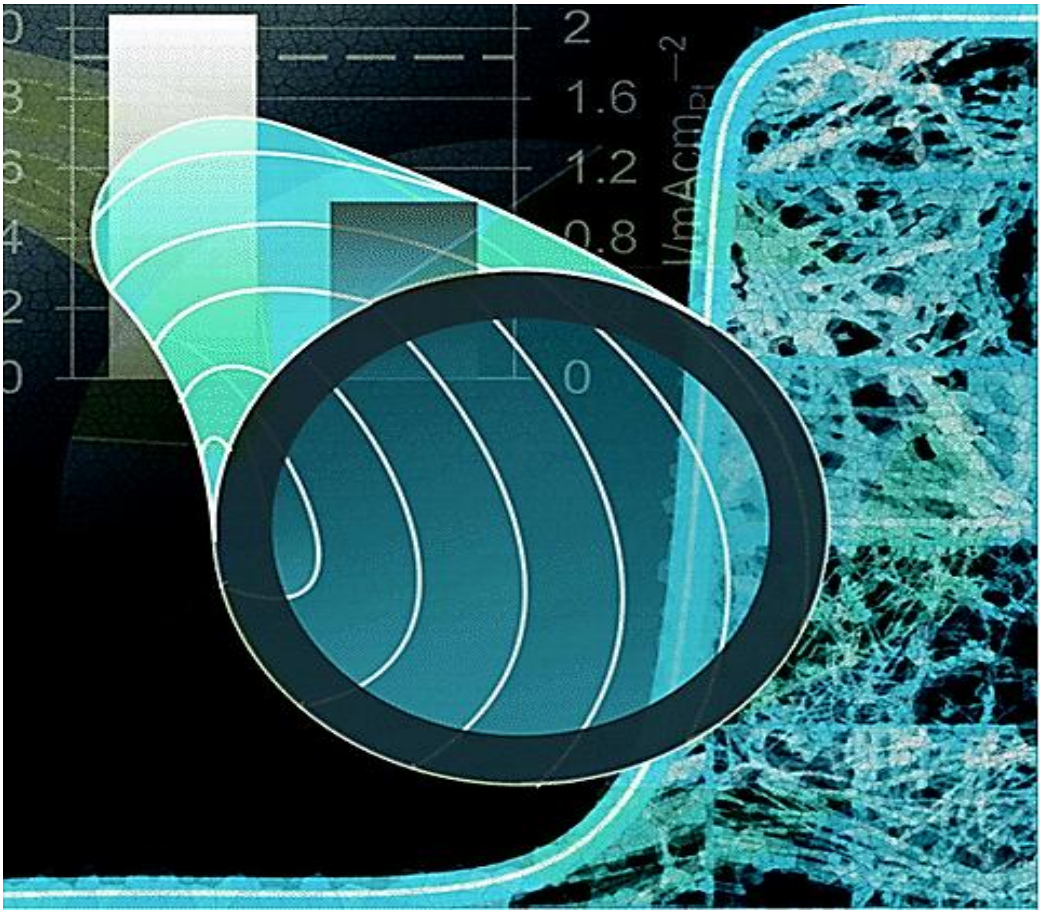

Fig 8 Platinum (Pt) coated palladium (Pd) nanotubes (Pt/PdNTs) with a wall thickness of 6 nm, outer diameter of 60 nm, and length of 5-20μm are synthesized via the partial galvanic displacement of Pd nanotubes[18].

1.2.2.2 Platinum-transition metal alloys

Zhu et al. have also prepared core shell FePtCu nanorods by the thermal decomposition of iron pent carbonyl and metal acetylacetonates. In this process, oleylamine and sodium oleate were used to control the growth of nanorods, while the growth of ternary nanorods were controlled by the precursor ratios.The synthesised samples had better stability especially in acid solution compared to that of binary counterparts. It provides an access to producing high efficient catalysts[19].

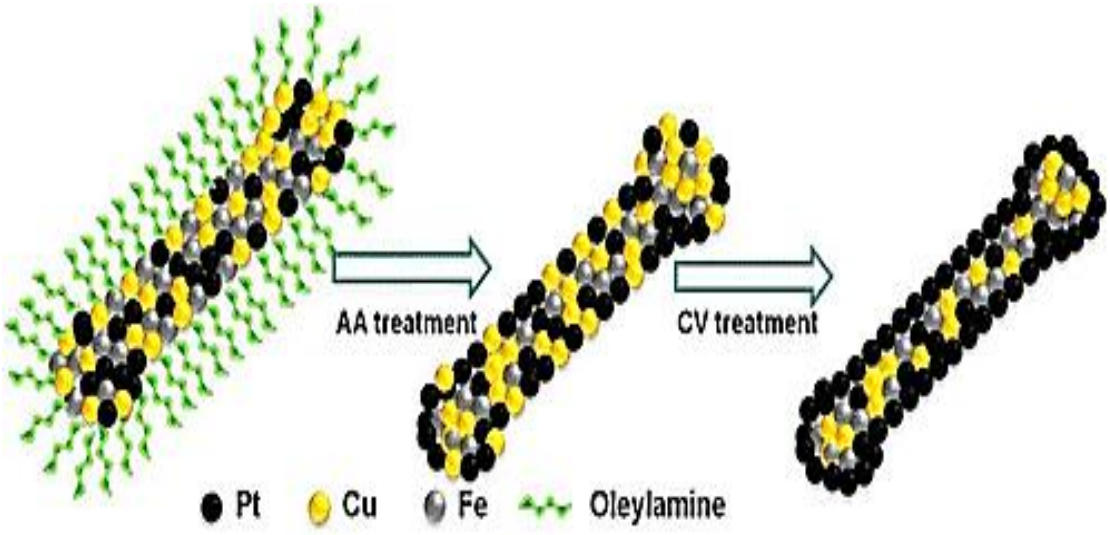

Fig 9 Synthesis of a new class of 20 nm × 2 nm ternary alloy FePtM (M = Cu, Ni) nanorods (NRs) with controlled compositions[19]

1.3 Carbon Nanotubes

1.3.1 General Description

Carbon nanotubes (CNTs) are seamless cylinders composed of one or more curved layers of graphene with either open or closed ends[20, 21]. There are classified as three types, that is, SWCNTs, DWCNTs and multiwall carbon nanotubes (MWCNTs).

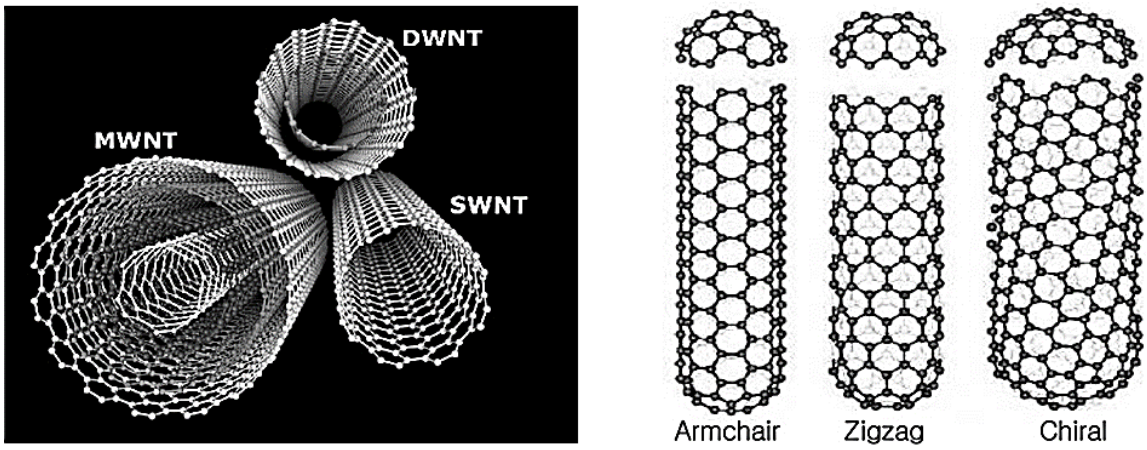

Fig 10Type of carbon nanotubes[20, 21]

1.3.2 General Functions

Afterthe find of CNTs in the year 1991[20], tons of research have been conducted in various areas[22-25]. The detailed information is not discussed in this paper. In the following discussion, the main topic is about the effect of the wall of carbon nanotubes on the catalytic activity of various catalysts.

1.3.3 Application in Oxygen Reduction Reaction

It is well acknowledged that CNTs have the benefits of good stability and electrochemical performance.In the past decades, noble and non-noble metal NPs supported on CNTs with enhanced activity for ORR were intensively studied in the past decades [26-31]. By synthesising transition metals doped onto various types of carbon nanotubes, the electro catalytic activity of prepared samples has been improved. Meanwhile, there is a strong affinity between transition metals and carbon nanotubes[32]. It is also believed that doping CNTs with heteroatom such as nitrogen[9, 33], boron[34], sulphur[35] and phosphorus[36] can dramaticallyenhance the performance. Miller et al. proved that the defects of SWCNTs generated by special treatment could also enhance the performance[37].

1.4 Recent Research

As this research focuses on the effect of the wall of carbon nanotubes on the performance of Pt nanoparticles, the following content will focus on the work that has done by our research group.

1.4.1 Pristine CNTs for Oxygen Evolution Reaction

There are seven types of carbon nanotubes used in this research from CNT-1 to CNT-7. The average numbers of walls of various carbon nanotubes are 1, 2, 3, 3, 7, >12 and >30, respectively. The TEM analysis results are shown in Figure 11 and Raman spectra analysis results are shown in Figure 12. The relevant data about various types of carbon nanotubes are also calculated through BET. The surface areas for CNTs are 651, 679, 643, 459, 485, 174, 85m^2 g^{-1}, respectively. The following research is mainly based on these carbon nanotubes.

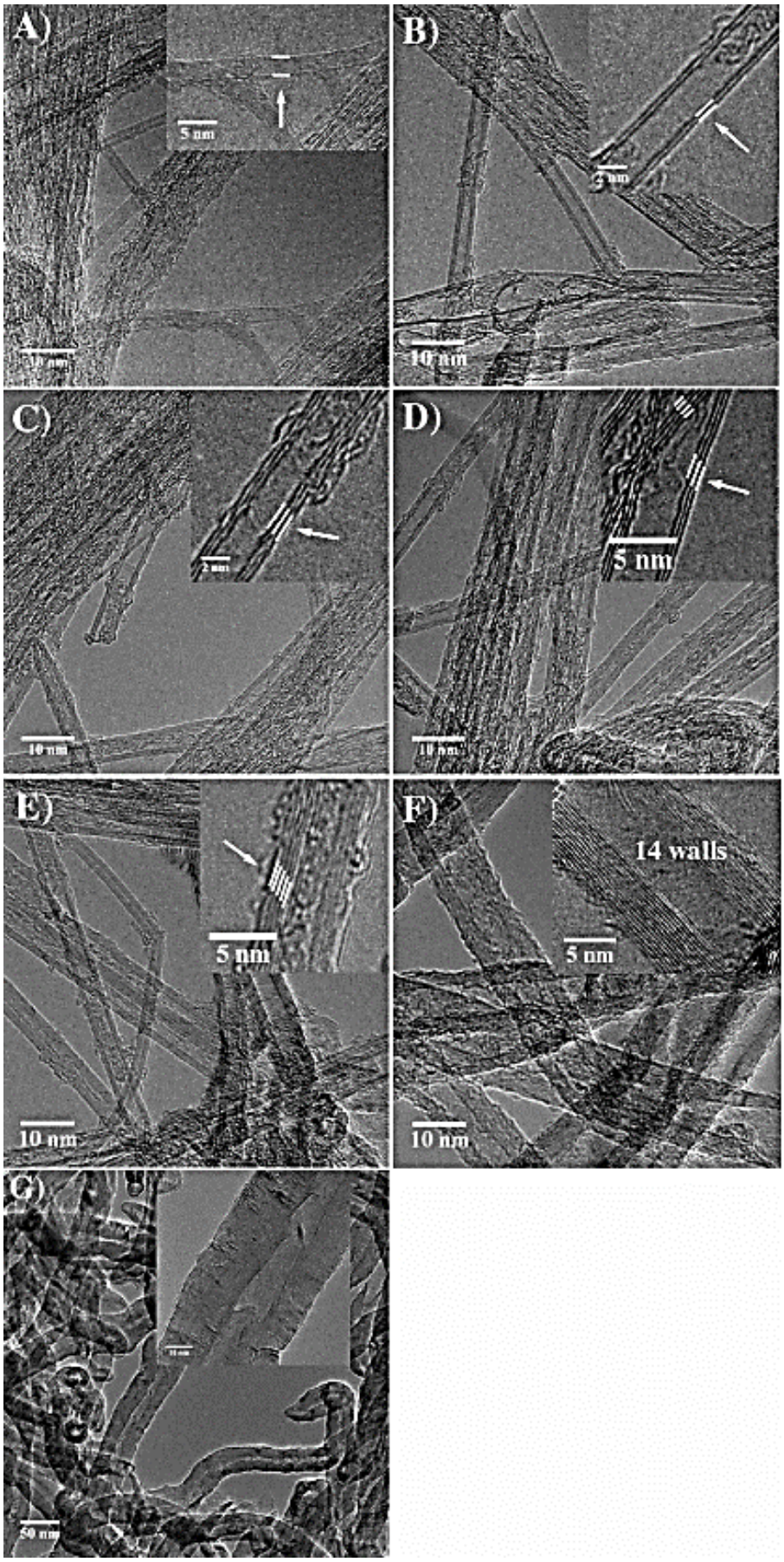

Fig 11 TEM analysis of CNTs

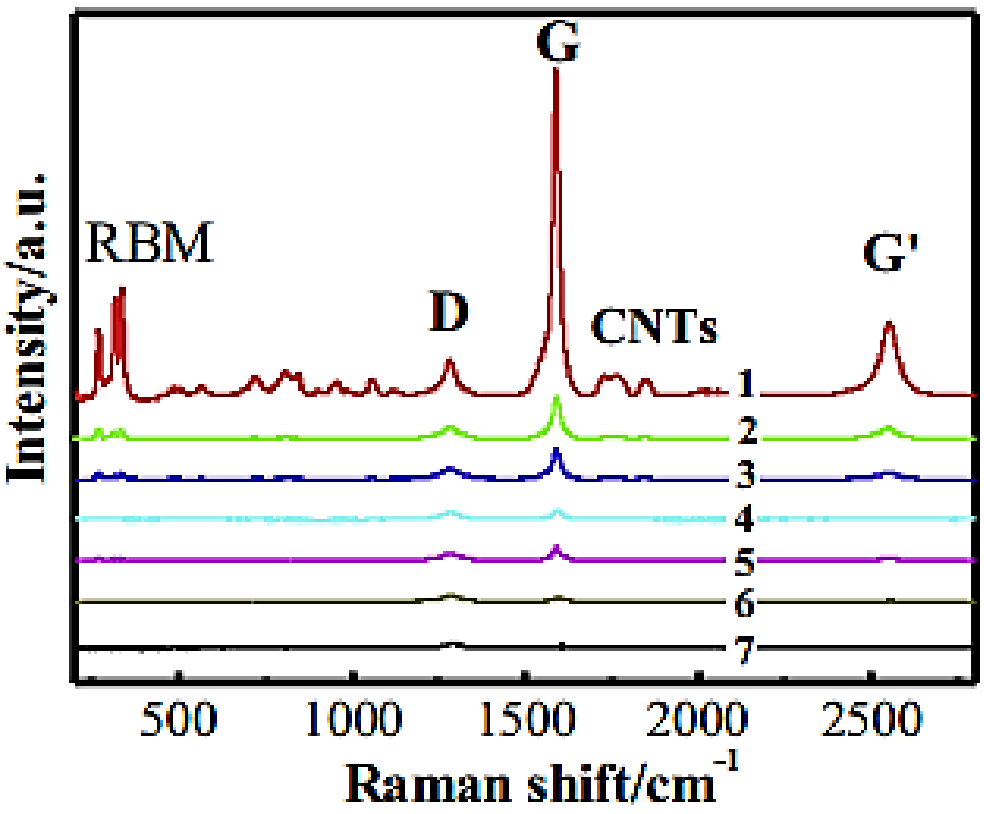

Fig 12 Raman spectra of CNTs

Then, these CNTs were washed and filtered by HCl for three days. Through TGA test, the amount of impurities was decreased significantly, as shown in Figure 13. Actually, the electro catalytic activity of various types of CNTs was not changed after the purification treatment, as shown in Figure 14. So, the impurities left were not the main factor for the electrochemical performance differences.

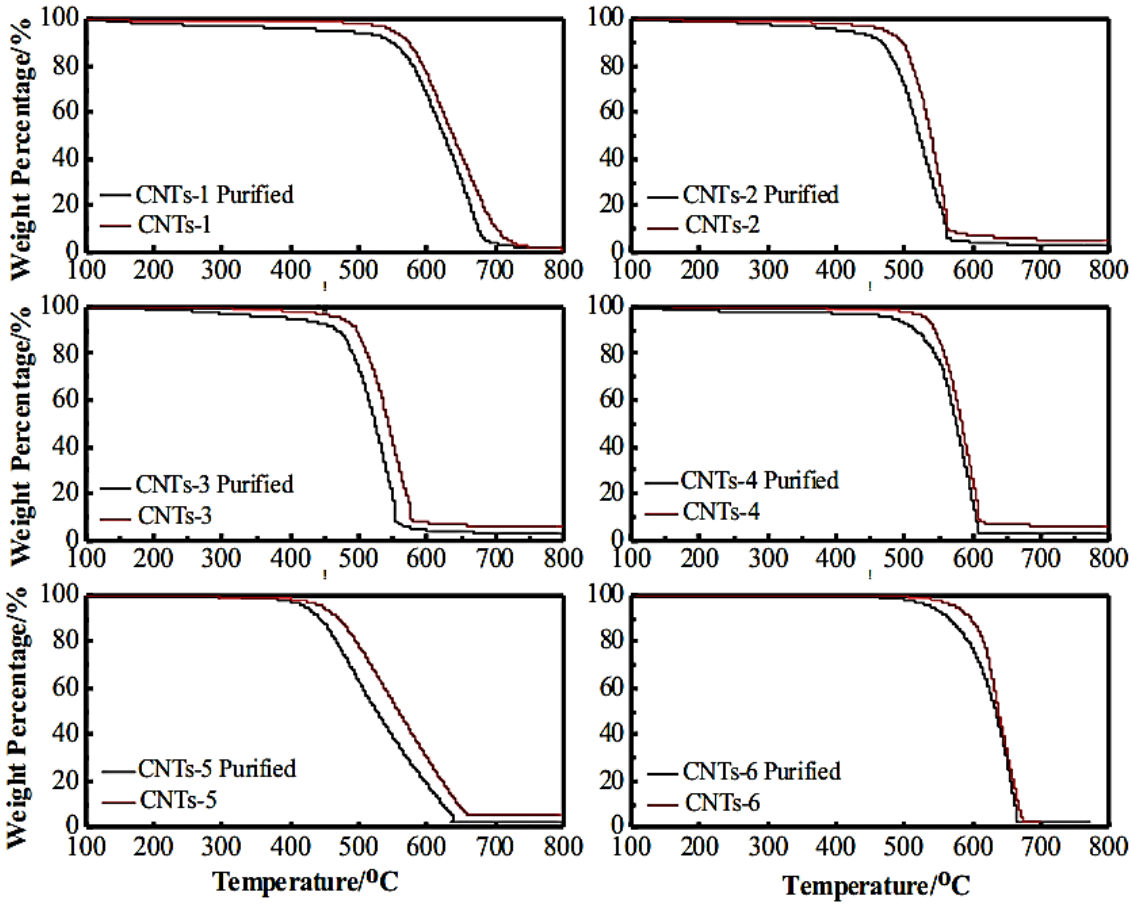

Fig 13 TGA analysis of CNTs

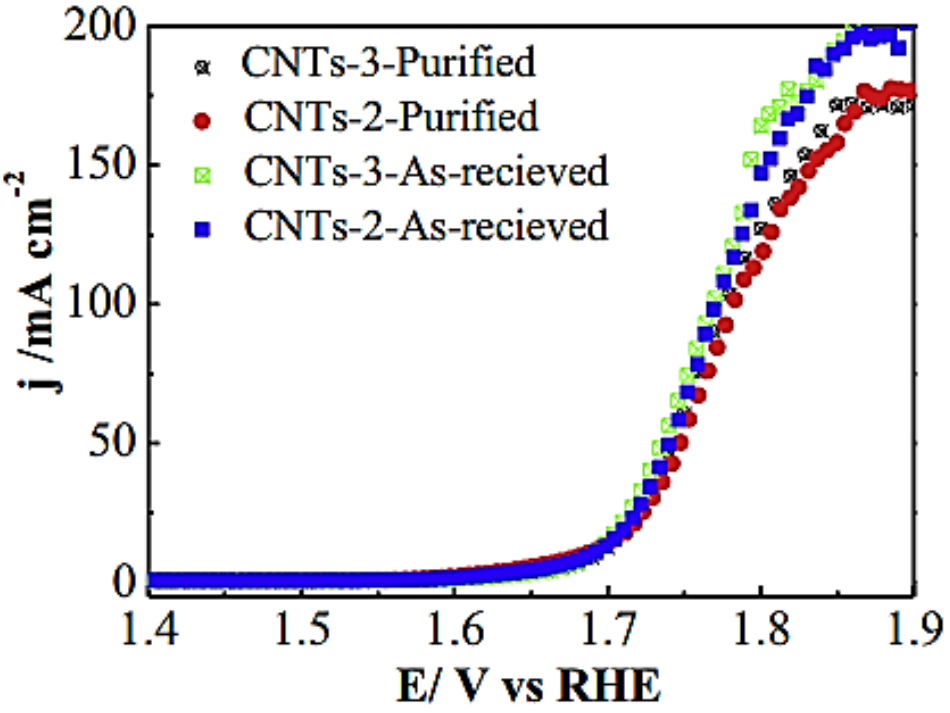

Fig 14 LSV of CNTs before and after the purification

After that, the performance of various types of CNTs was tested, including the TOF and chronopotentiometry. The activity was also concluded in Figure 15-17. The electrochemical activity of triple wall carbon nanotubes was better than that of other types of CNTs.

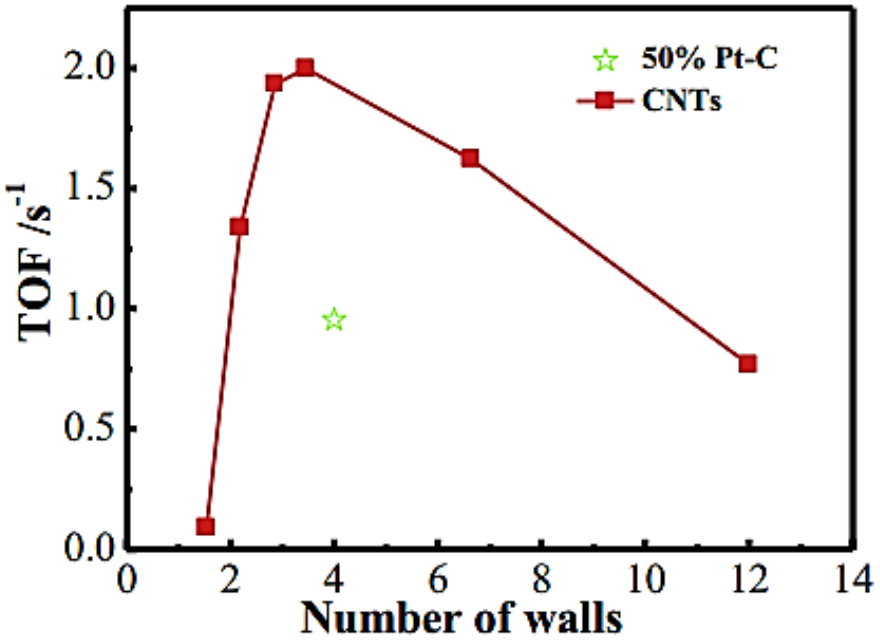

Fig 15 the TOF vs the wall numbers of CNTs

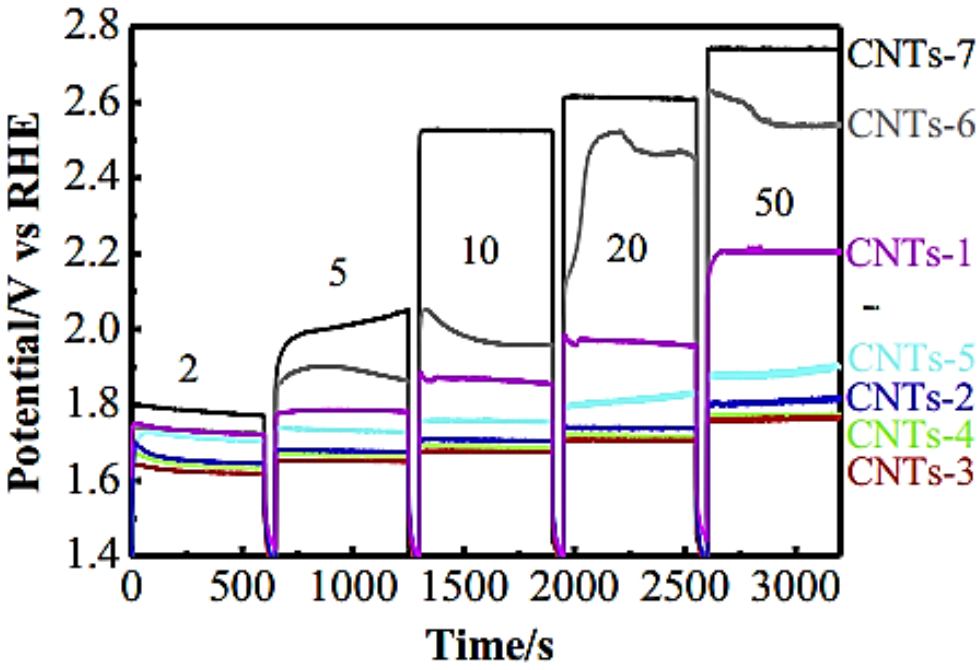

Fig 16 Chronopotentiometry curves of CNTs

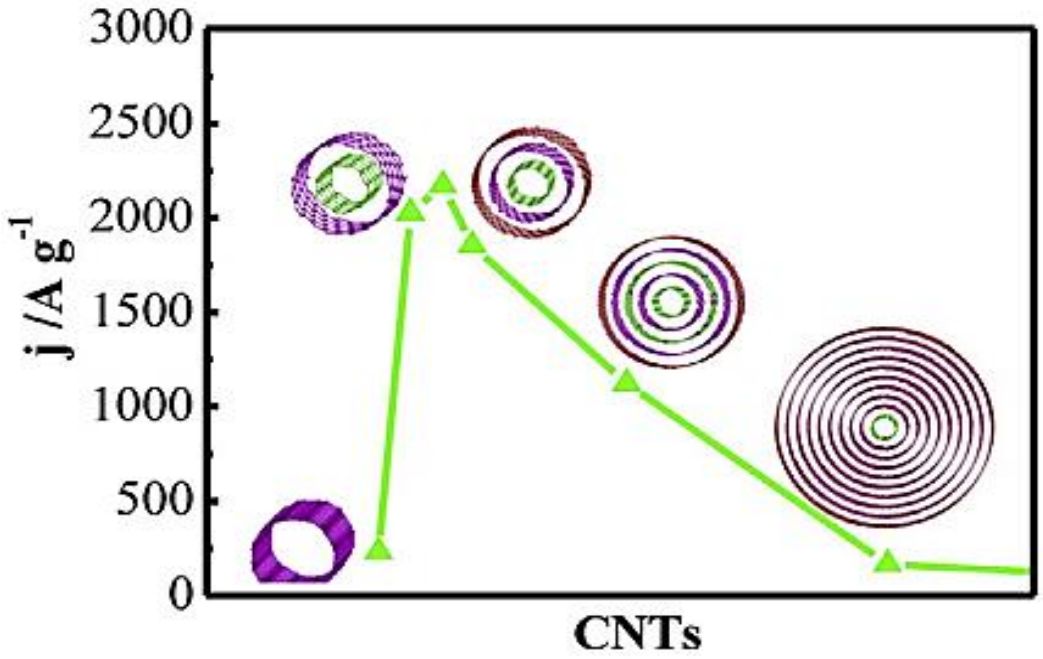

Fig 17 Plot of the activity of CNTs for the OER

In order to explain this phenomenon, one hypothesis is proposed. The reason for the better performance is due to the quantum effect of double and triple wall carbon nanotubes. The outer wall is reaction site, while the inner wall is useful for fast electron transfer. As for single wall carbon nanotubes, there is no quantum effect. When it comes to MWCNTs, the effect is decreased with increased wall numbers.

1.4.2 Pd/CNTs for Ethanol Oxidation

There are four types of carbon nanotubes used in this research that is CNT-1, CNT-2, CNT-5, and CNT-6. The average numbers of walls of various carbon nanotubes are 1, 2, 7, and 12, respectively. The TEM analysis results are shown in the aforementioned discussion. The relevant data about various types of carbon nanotubes are also calculated through BET. Based on the N_2 adsorption isotherms the BET surface area of CNTs-1, CNTs-2, CNTs-5 and CNTs-6 is 576.7, 523.2, 538.8 and 270.6 $m^2 g^{-1}$, respectively.

In this research, Pd/CNTs were used as catalysts [38, 39]. Pd nanoparticles were homogenously dispersed onto the surface of CNTs and the Pd nanoparticle size was also similar. Through the following TGA test, the loading of Pd was the same as well.

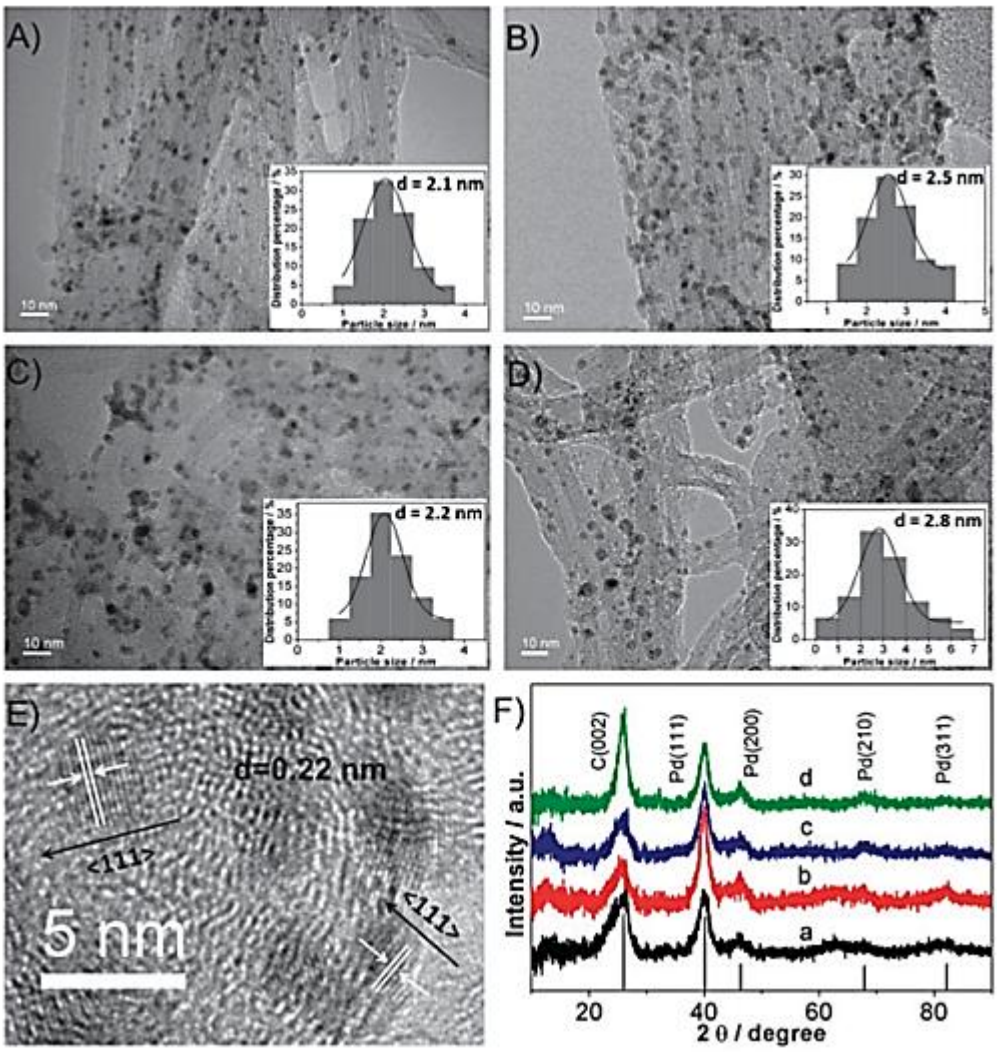

Fig 18 TEM images of Pd/CNTs

After that, the performance of various types of CNTs was tested, including the cyclic voltammetry. The activity was also concluded in Figure 19. The electrochemical activity of triple wall carbon nanotubes was better than that of other types of CNTs.

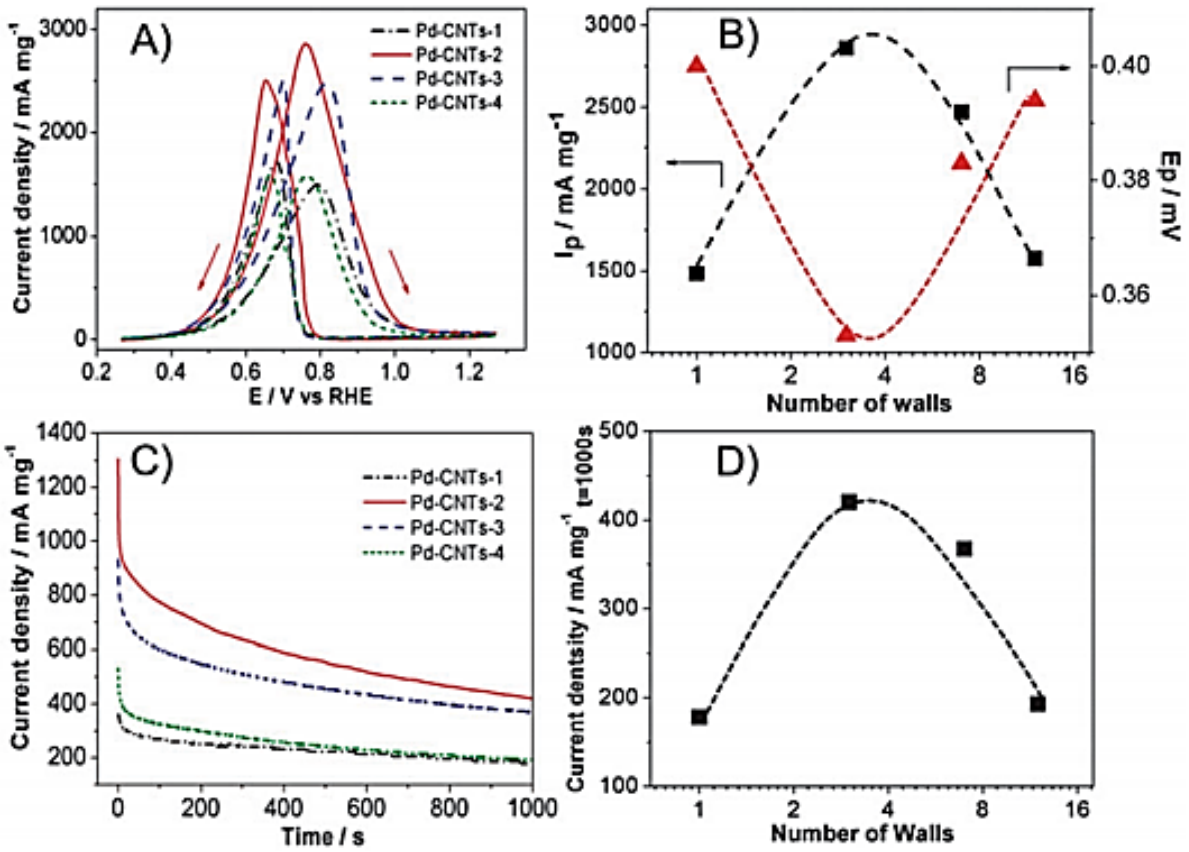

Fig 19 Cyclic voltammetry curves of various types of CNTs

In order to explain this phenomenon, one hypothesis is proposed. The reason for the better performance is due to the quantum effect, which has been presented in the aforementioned discussion.

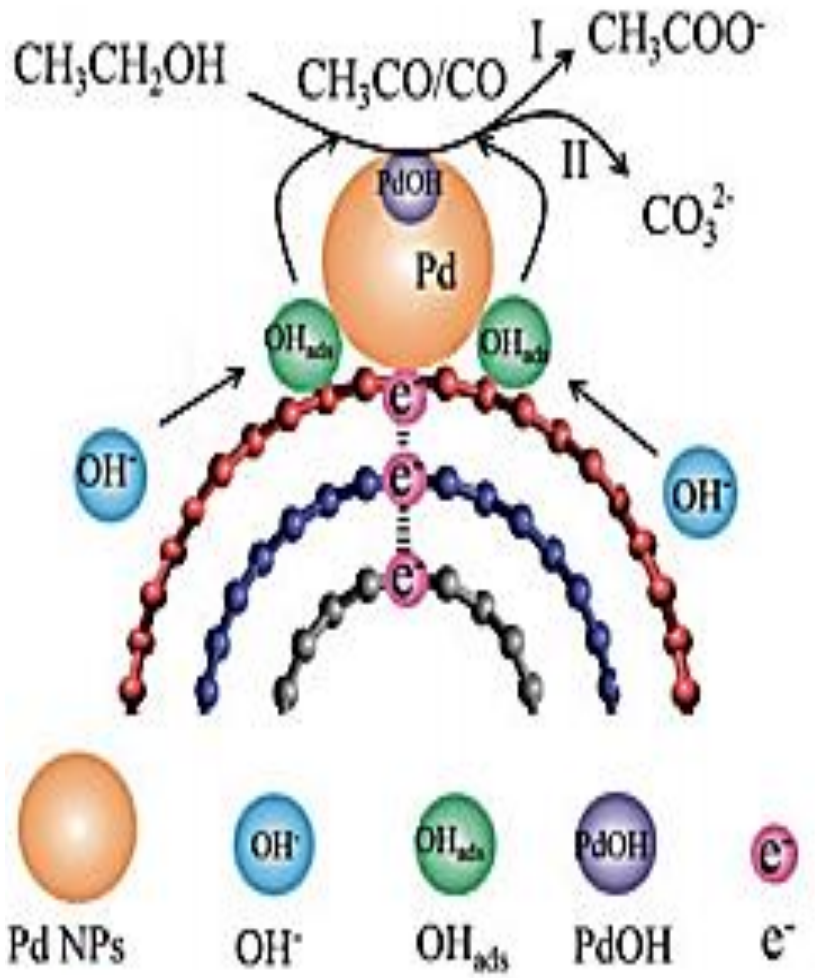

Fig 20Theoretic scheme of DWCNTs for EOR

1.4.3 Methanol/ Formic Acid Oxidation

There are six types of carbon nanotubes used in this research, including CNT-1, CNT-2, CNT-3, CNT-5, CNT-6, and CNT-7. The average numbers of walls of various carbon nanotubes are 1, 2, 3, 7, >12 and >30, respectively. The TEM analysis results and Raman spectra analysis results are shown in Figure 21.

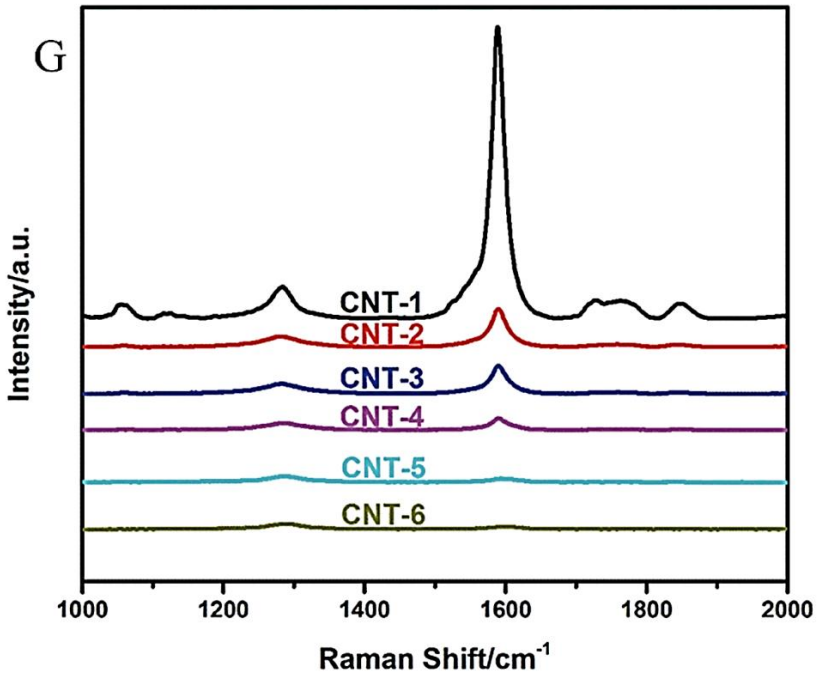

Fig 19 Raman spectra images of CNTs

In this research, Pd/CNTs were used as catalysts [38, 39]. Pd nanoparticles were homogenously dispersed onto the surface of CNTs and the Pd nanoparticle size was also similar. Through the following TGA test, the loading of Pd was the same as well.

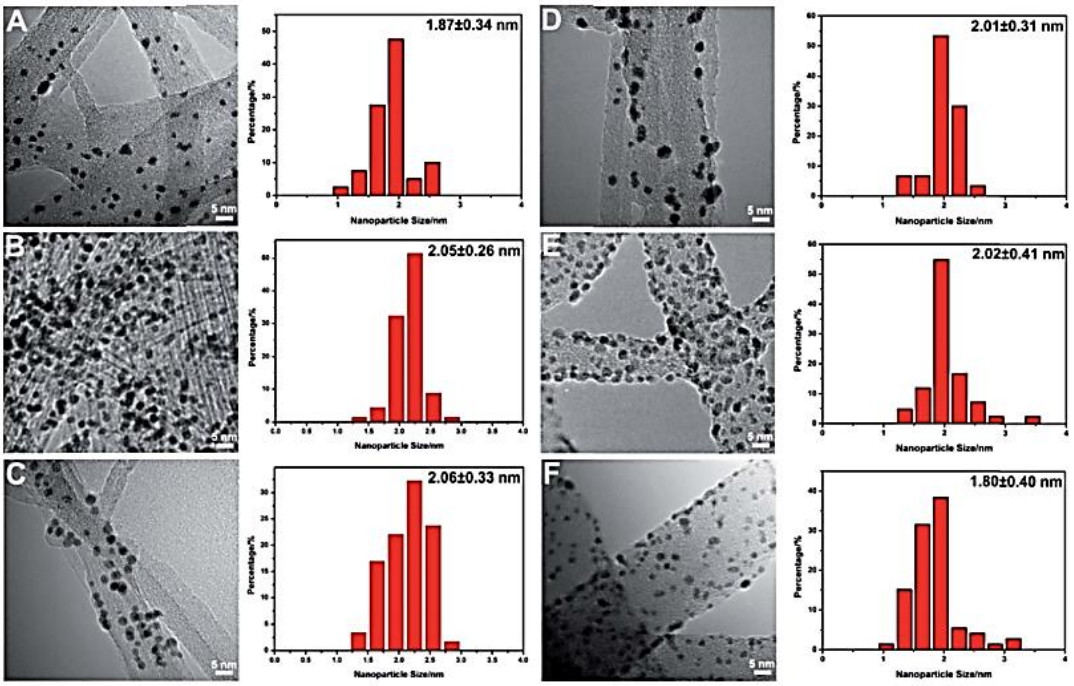

Fig 20 TEM images of Pd/CNTs

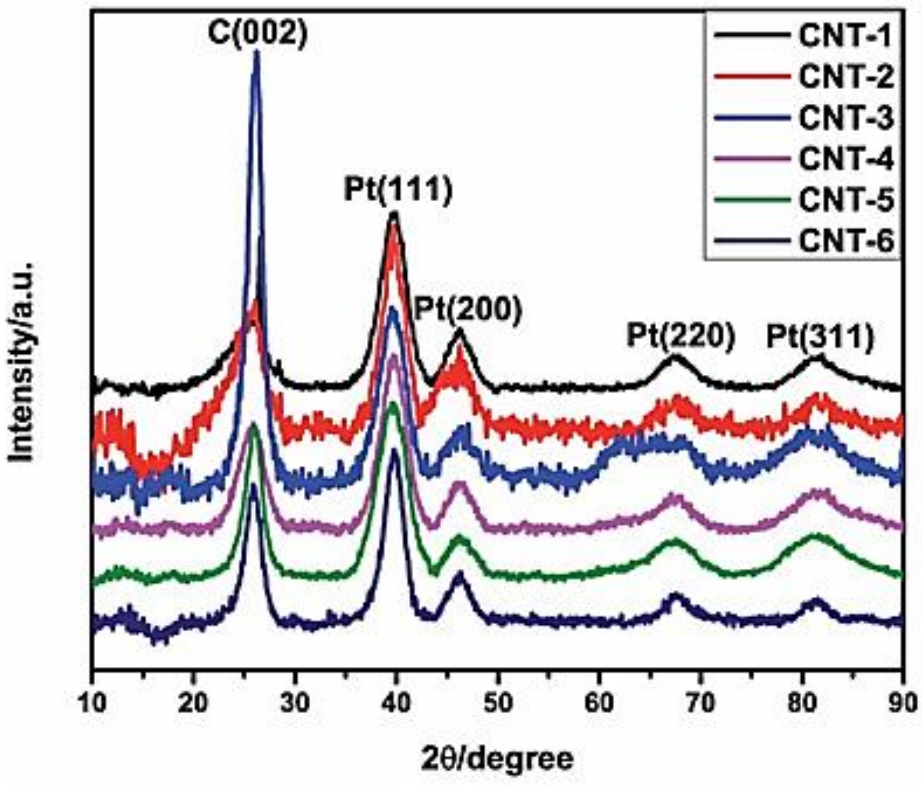

Fig 21 XRD images of Pd/CNTs

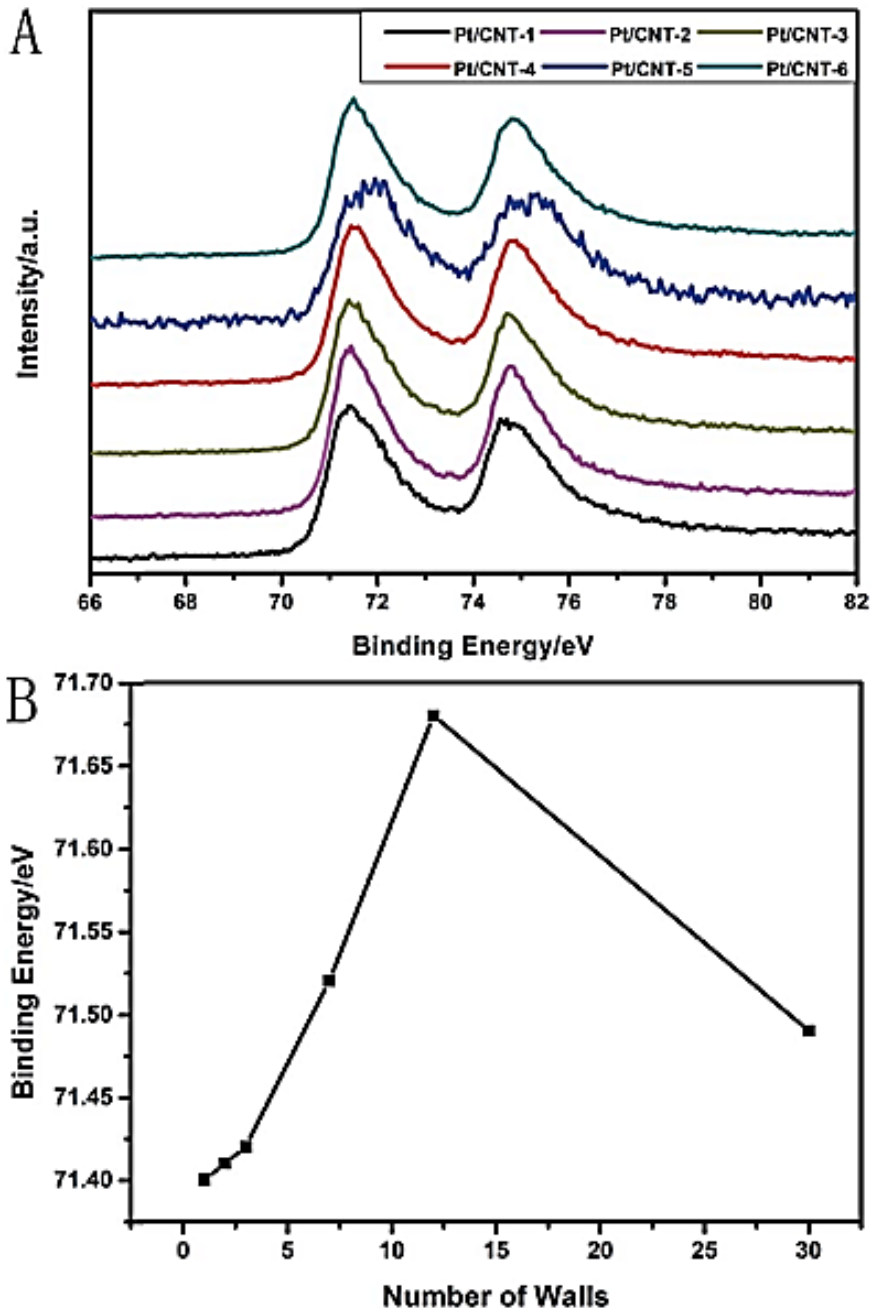

Fig 22 XPS and BE images of Pd/CNTs

After that, the performance of various types of CNTs was tested, including the TOF and chronopotentiometry. The activity was also concluded in Figure 25. The electrochemical activity of triple wall carbon nanotubes was better than that of other types of CNTs.

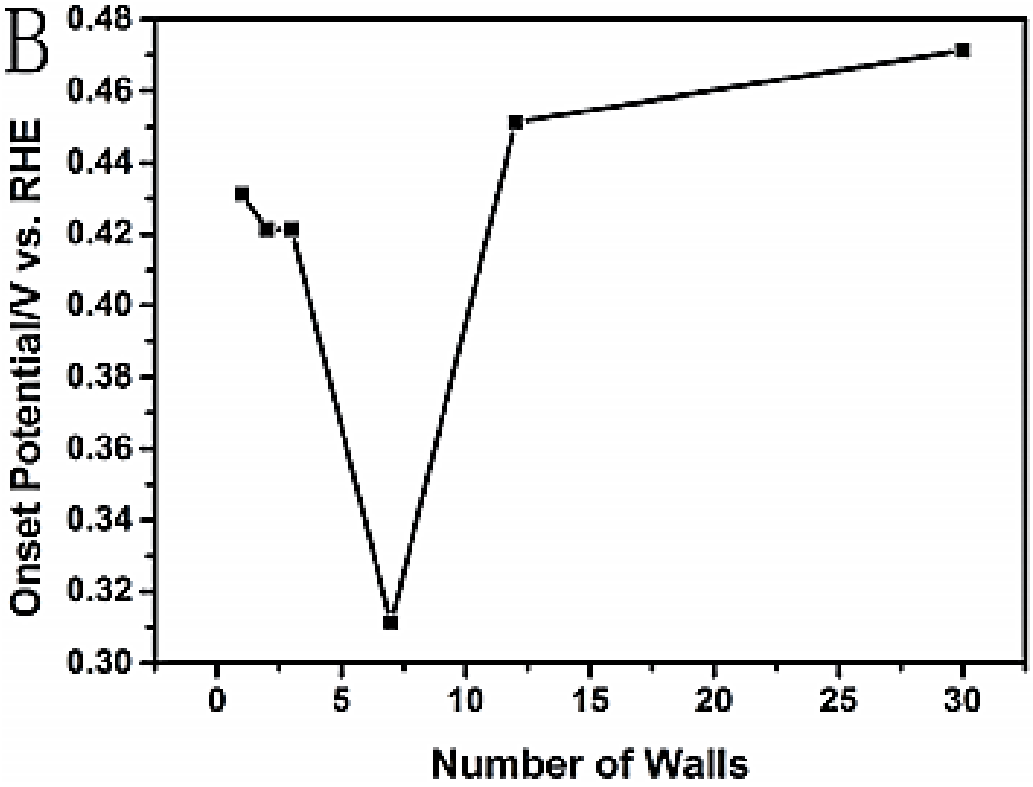

Fig 23 Onset potential of CO oxidation of CNTs

In order to explain this phenomenon, one hypothesis is proposed. The reason for the better performance is due to the quantum effect, which has been presented in the aforementioned discussion.

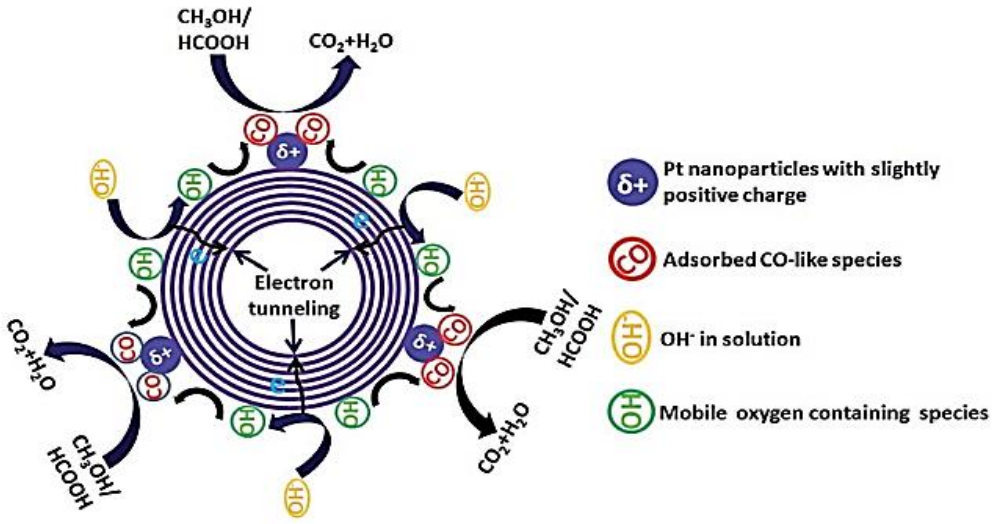

Fig 26Schematic diagrams presenting the promotion effect the CNT support

1.4.4 Dye Functionalized Carbon Nanotubes for Photoelectrochemical Water Splitting[40]

There are seven types of carbon nanotubes used in this research from CNT-1 to CNT-7. The average numbers of walls of various carbon nanotubes are 1, 2, 3, 3, 7, >12 and >30, respectively. The TEM analysis and Raman spectra analysis results are shown in Figure 27. In this paper, we reported that CNTs composed of 2-3walls are better supports for Pt NPs to wire-up ORR reaction in alkaline conditions.

After that, the performance of various types of CNTs was tested, including the photo-current density. The activity was also concluded in Figure 28. The electrochemical activity of triple wall carbon nanotubes was better than that of other types of CNTs.

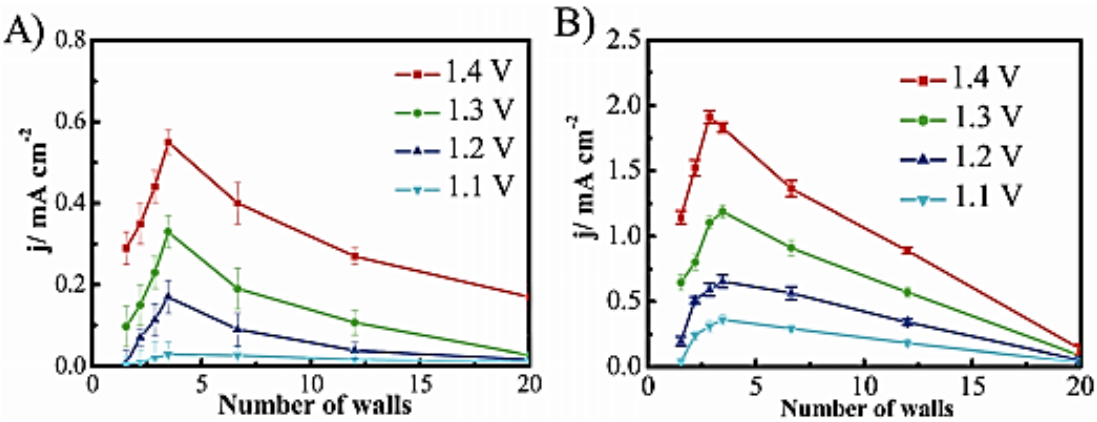

Fig 24 TEM images of CoPc/CNTs and Rubpy/CNTs

In order to explain this phenomenon, one hypothesis is proposed. The reason for the better performance is due to the quantum effect, which has been presented in the aforementioned discussion.

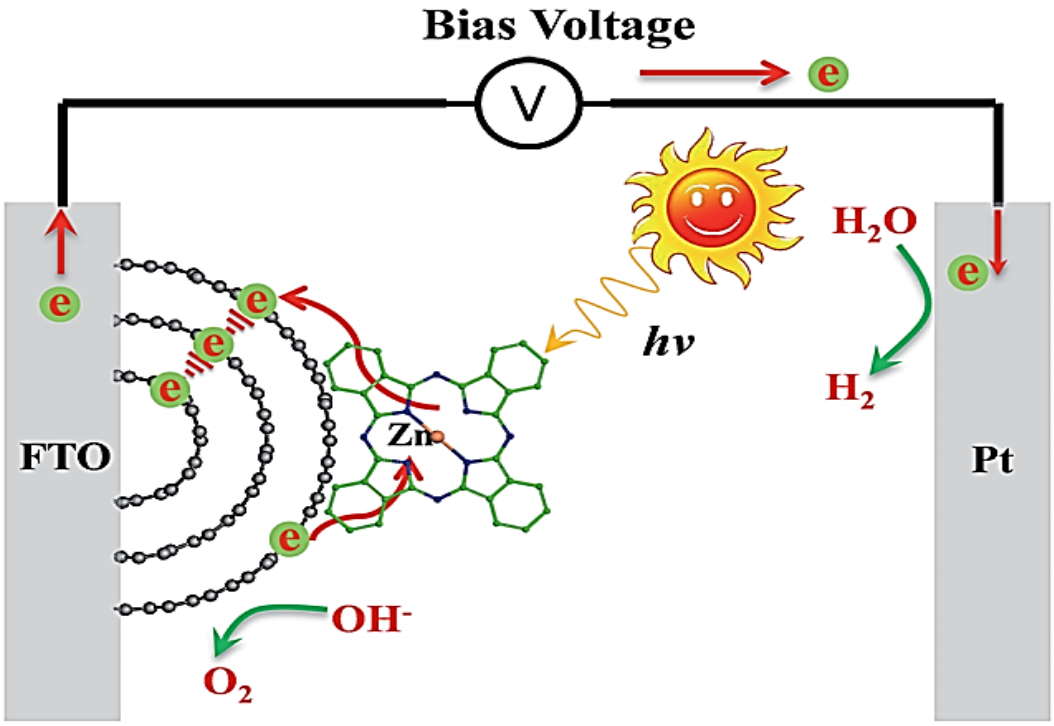

Fig 28 Scheme of ZnPc/CNTs for PEC water oxidation

2 Experiments

2.1 Materials

Four types of CNTs were prepared from commercial sources.CNTs with different number of walls and diameters were obtained from commercial sources including Nanostructured & Amorphous Materials, Inc.,USA(SWCNTs), Beijing Dk Nano Technology Co., LTD, China and Shenzhen Nano, China (DWCNTs & MWCNTs). 50mg of CNTs were washed and filtered with 37 wt % of HCl for three times for eliminating impurities while synthesis process. Other materials include Potassium hexachloroplatinate (IV) acid, Polyethylenimine (PEI), Potassium hydroxide (KOH), Perchloric acid (70 wt %), Ethanol, Nafion, which were purchased from Sigma-Aldrich.

2.2 Preparation of Pt /CNTs

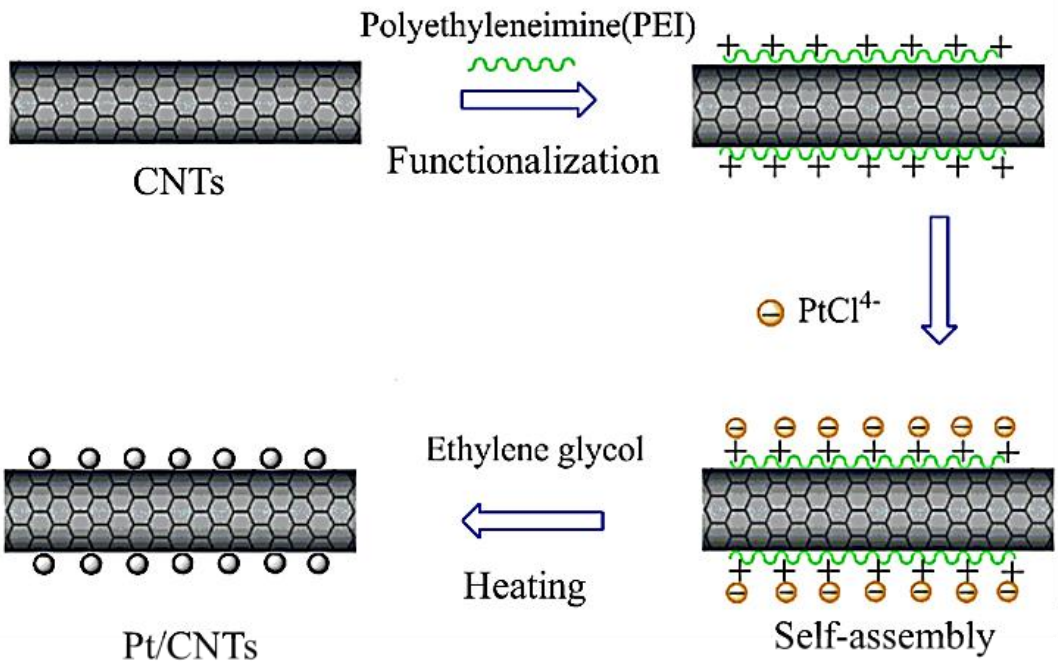

Fig 29 Procedure for the preparation of Pt/CNTs

20%Pt/CNTs: Pristine CNTs (100 mg) were functionalized using PEI following the procedures reported elsewhere[41], which was named as Pt/CNTs. 40 mg PEI/CNTs were ultra-sonicated in 240 mL ethylene glycol(EG) solution for 1hour.

Then, a certain amount of $K_2PtCl_6$was added and heat treated at 150 ^oC for 3 hours.After that, the solution was cooled in the ambient environment and then dried overnight at 70 ^{o}Cunder vacuum. The product was noted as Pt/CNTs, shown in figure 30.

2.3 Characterization

In this study, the loading of Pt onto the surface of carbon nanotubes was tested by TGA (Q5000, USA). The surface area of four types of CNTs was measured by A Micromeritics Tristar II 3020 instrument in order to confirm the type of CNTs. And the XPS(Kratos AXIS Ultra DLD) wasapplied to confirm the state of Pt, which was also confirmed by XRD (Rigaku D/MAX RINT 2500) test. The morphology of Pt nanoparticles was tested by TEM analysis (JEOL3000) with operating at 300 kV.

Typical three electrode cell was used to measure the electrochemical catalytic activity of prepared Pt/CNTs. All potentials in the present study were given versus RHE reference electrode: $E=E_{SCE} + E_{SCE} + 0.059 \times pH$, where $E_{SCE} = 0.247$ vs. RHE at 20^{o}C. The electrochemical active of functionalized CNTs and Pt/CNTs were measured in an oxygen saturated 0.1 M KOH and 0.1M $HClO_4$ solution at a scan rate of 10 mV s^{-1} for linear sweep voltammetry (LSV). As for LSV test, parameters were scan rate10 mV s^{-1}, stirring rate1600 rpm and catalysts loading of 0.031 mg cm^{-2} in Hydrogen chloride(HCl) or KOH solutions.

2.4 Data Management

Linear sweep voltammetry [42], cyclic voltammetry, electron transfer numbers[43], current exchange density[43], chronoamperometry[44]and Tafel slop[45] are commonly used for comparison of the electrochemicalcatalyticactivity. In this research, LSV, electron transfer number and Tafel slop will be applied for the comparison of the performance of Pt/CNTs.

3 Results

3.1 Characterizations of CNTs

TEM micrographs of CNTs after purification by washed with 30 wt% HCl three times. In order to calculate the average number of walls and outer diameter (OD) in various CNTs, over one hundred images of CNTs were selected[46]. CNTs-1 is mainly of SWCNTs (79%) with OD of around 2.0nm. CNTs-2 is mainly of DWCNTs (65%) with OD of about 3.3nm. CNTs-3 and CNT-4 are typical MWCNTs with average number of walls of 12 and 30 and OD of about 13.9nm and 35.2nm, respectively. All relevant parameters are calculated as shown in Table 1.

Table 1the basic parameters of four types of CNTs

CNTs	CNT-1	CNT-2	CNT-3	CNT-4
Number of walls	1(79%) 2(16%) 3(5%)	2(65%) 3(23%)	>12	>30
Average number of walls	1	2	12	30
Overall outer diameter (nm)	2.0	3.3	13.9	35.2
Surface area (m^2 g^{-1})	651	679	174	264

Table2 indicates the basic parameters of various CNTs. According to the table, it is apparent that the average wall numbers of four types of CNTs were 1, 2, 12 and 30. Meanwhile, the overall outer diameters were increased with increased wall numbers, while the surface areas were decreased.

3.2 Characterizations of Pt/CNTs catalysts

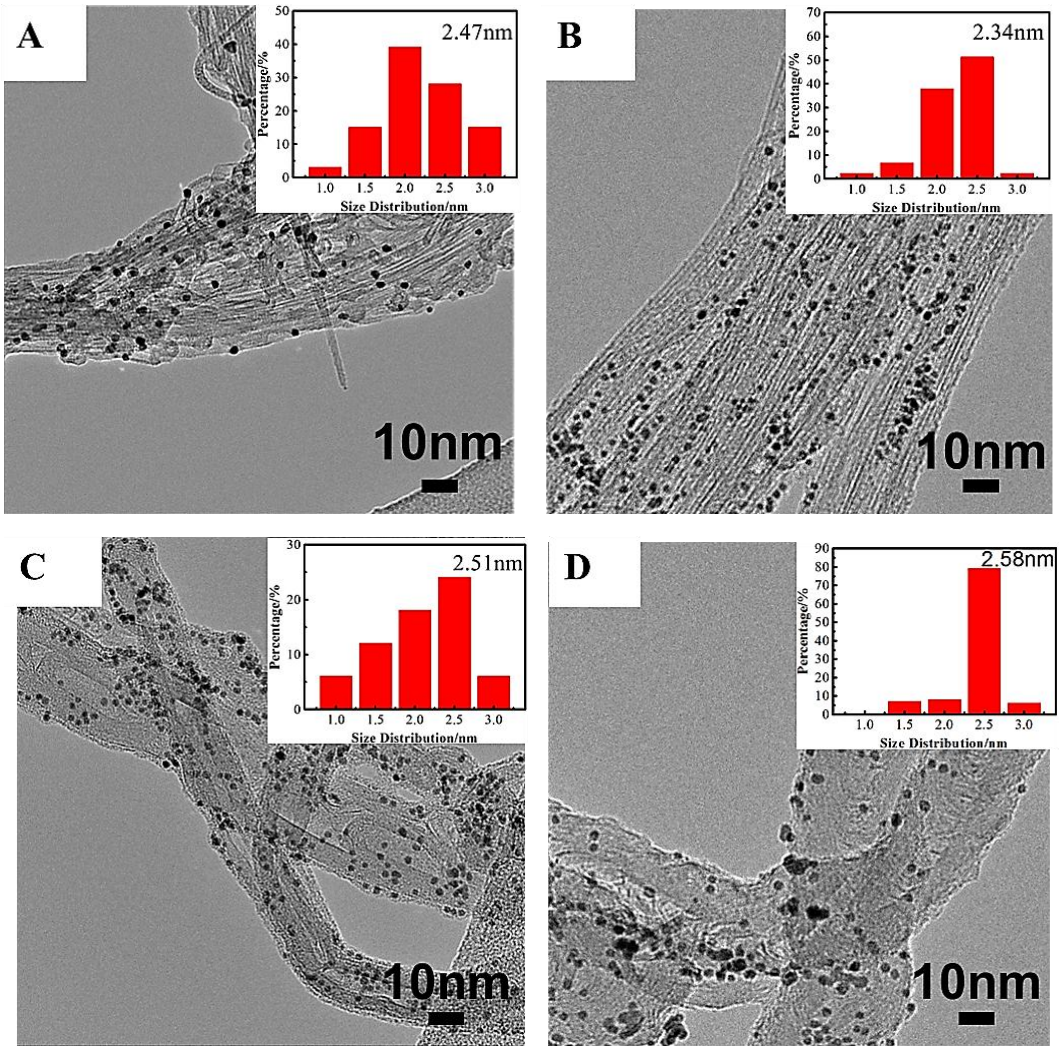

Fig 25 TEM analysis of the Pt/CNTs

Fig. 30 indicates TEM images of Pt/CNTs. Pt NPs are homogeneouslydispersed on the CNTs with a small range of size from 2.34nm to 2.58nm. PEI is essential for modification of the surface of CNTs for uniform loading of $PtCl^{4-}$ NPs[47]. The negatively charged sidewall of CNTs is easily wrapped by cationic polyelectrolyte PEI by electrostatic attraction. After the addition of K_2PtCl_6 solution, the N atoms are easily to coordinate with $PtCl^{4-}$ ions. Eventually, chemical reduction of Pt NPs would attach on the surface of CNTs. Without the functionalization of PEI, there would be no Pt NPs decorated on the surface and CNTs would be bare as well. The small range of Pt nanoparticle size is mainly contributed to the ratio of ethylene glycol−water ([48].

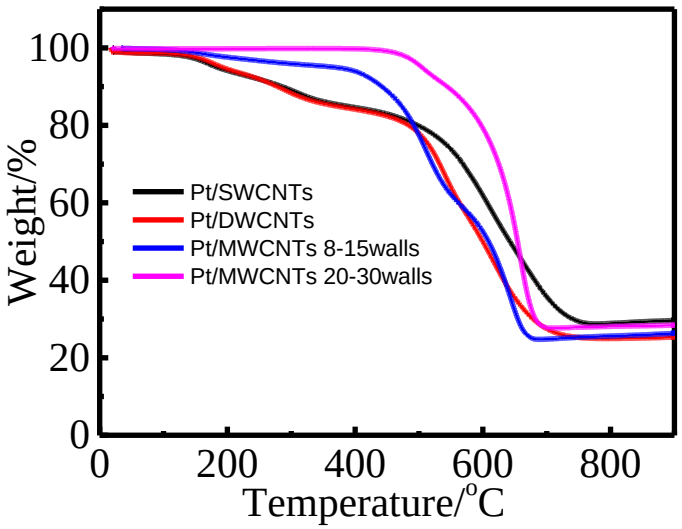

Fig 26 TGA analysis of the Pt/CNTs

The weight percentage of Pt loading on CNTs was measured by TGA test. As shown in figure 31, the weight loss is about 25% in the case of Pt/CNTs, with Pt/CNTs-1 23%, Pt/CNTs-2 25%, Pt/CNTs-3 28% and Pt/CNTs-4 27%. This means the loading of Pt on these kinds of composite is approximately 25%. The TGA results indicated thatPt was successfully deposited, which is consistent with TEM test results.

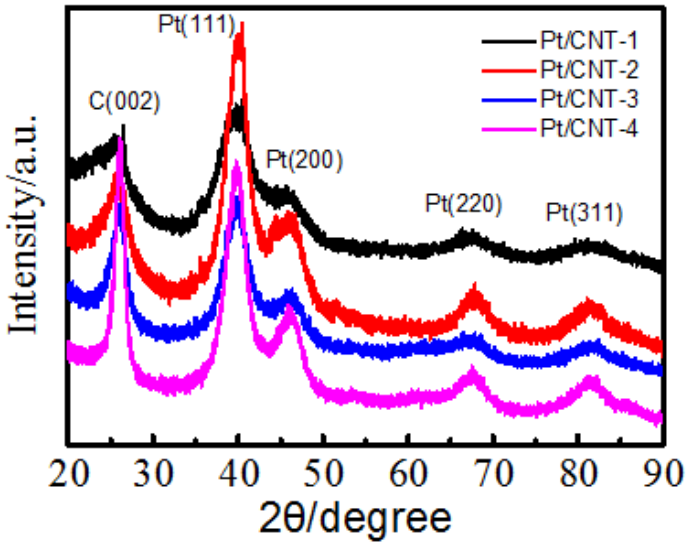

Fig 27 XRD analysis of the Pt/CNTs

Fig. 32demonstrates the XRD patterns of the Pt/CNTs. The calculated sizes of

the Pt nanoparticlesdoped onto the surface of CNT-1, CNT-2, CNT-3 and CNT-4 were close, varying from 2.48 to 3.31 nm.The calculated size of Pt nanoparticleswaslarger than that of TEM analysis as shown in Table 3.

Table 2Particle sizes of Pt nanoparticlesdoped onto various CNTs

Parameter	Catalyst Types			
	Pt/CNTs-1	Pt/CNTs-2	Pt/CNTs-3	Pt/CNTs-4
Pt NP size (nm, TEM)	2.47	2.37	2.51	2.58
Pt NP size (nm, XRD)	2.48	3.18	2.84	3.31

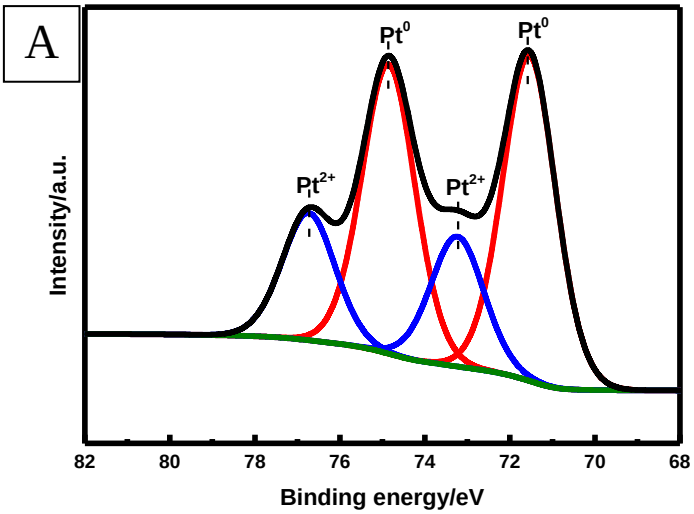

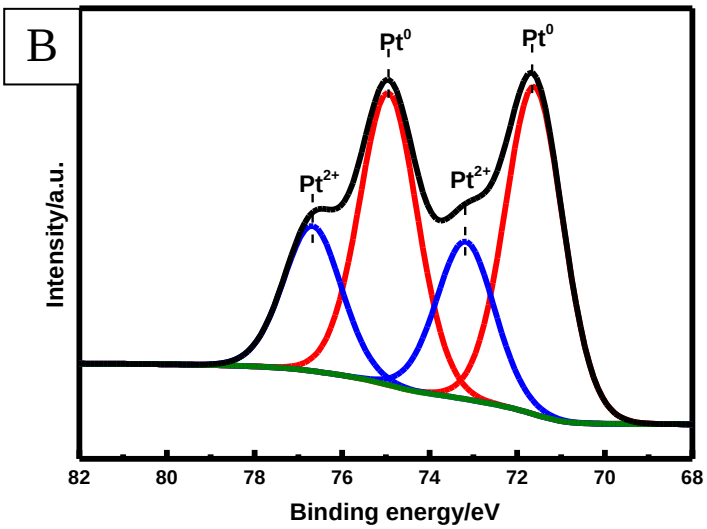

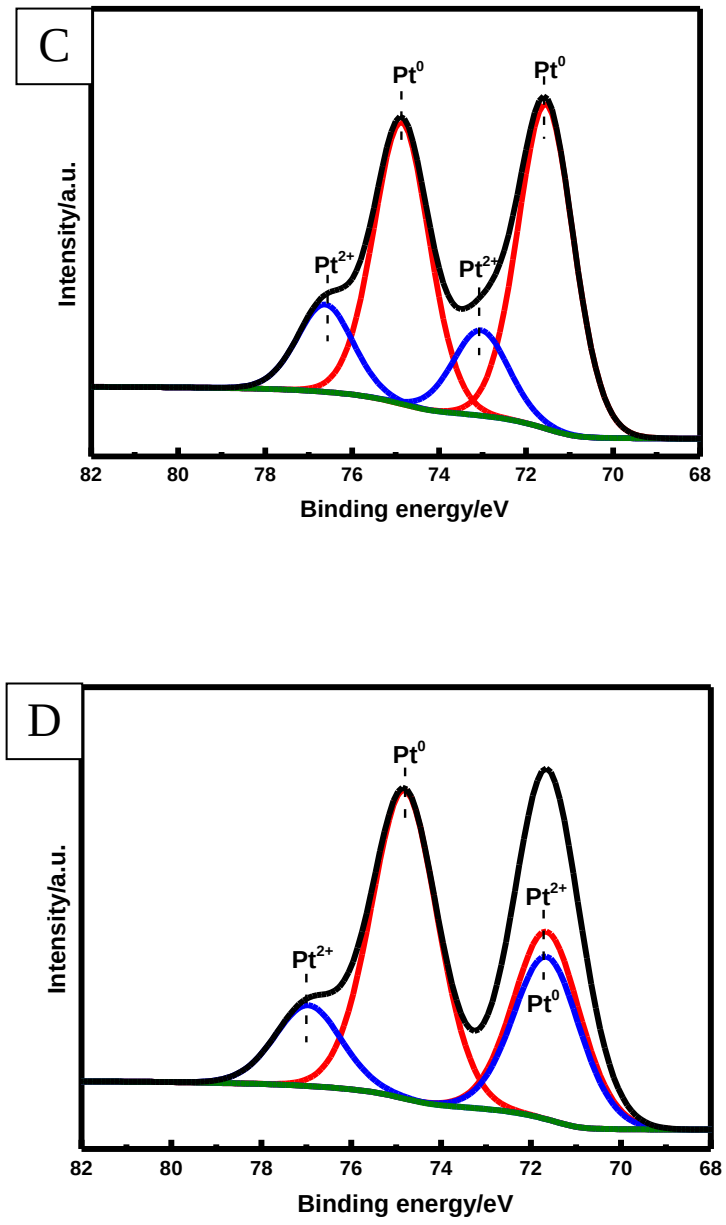

Fig 28XPS spectra of the Pt/CNTs

As shown in Fig 33, the XPS survey scan spectrum exhibits distinct Pt 4f peaks from Pt/CNTs. Specifically, two chemically different Pt entities could be identified as marked in the spectrum, corresponding to metallic Pt (0) with binding energies (BE) of 71.5 and 74.8 eV, and oxide Pt(II) with BE of 72.9 and 76.2 eV oxide.

Obviously, the anchored Pt species are predominantly in the metallic state, with Pt/SWCNTs (70.4%), Pt/DWCNTs (67.2%), Pt/MWCNTs-1 (77.8%), and Pt/MWCNTs-1 (67.1%), respectively.

3.3 LSV analysis of Pt/CNTs in alkaline solution

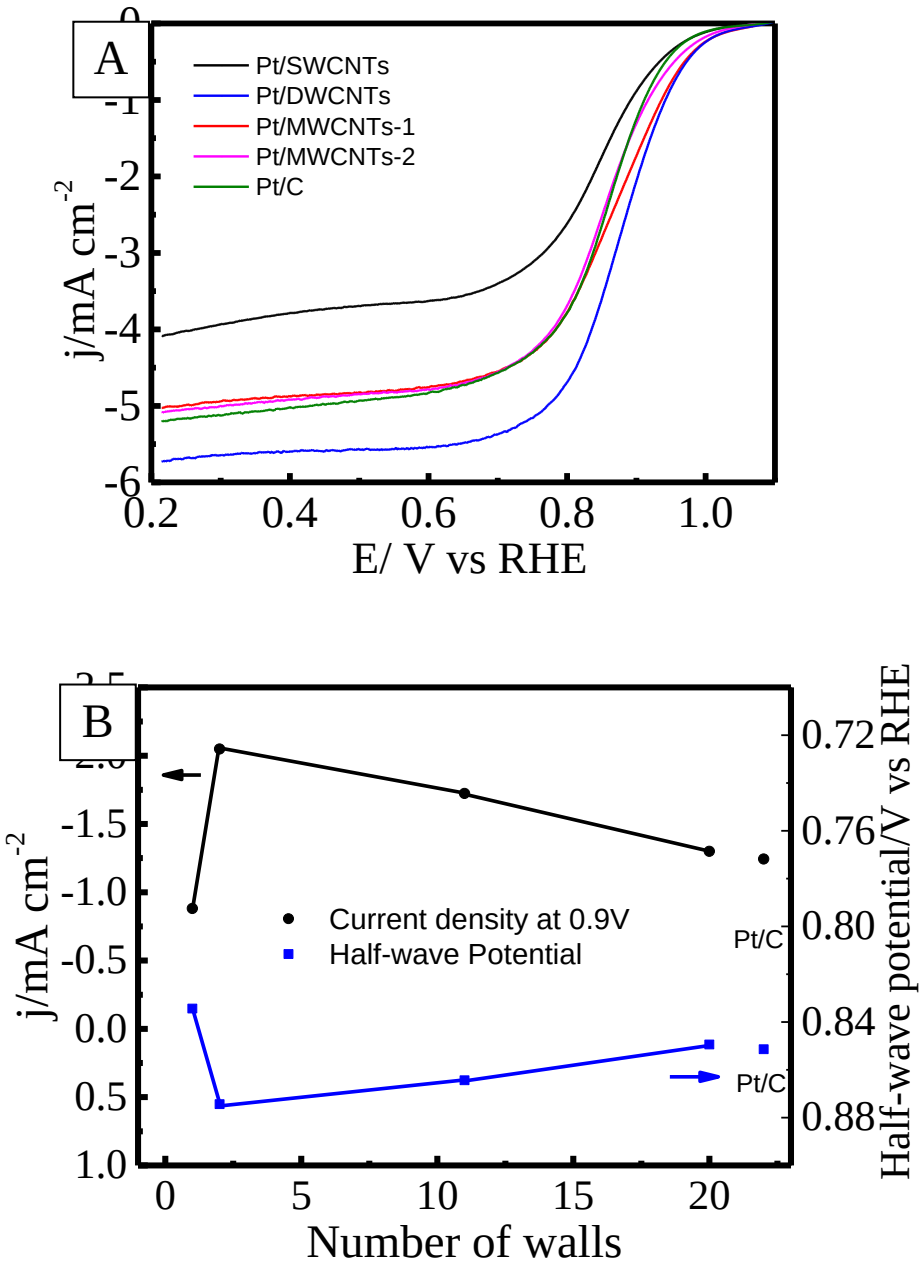

Fig 29A) Linear scan voltammetry of ORR. B) Current density at 0.9 V.

Figure 34 shows the LSV of ORR on Pt/CNTs electrode in 0.1 M KOH. The number of walls of CNTs has significant influence on the ORR. There was a volcano relationship between the current density and the number of walls in alkaline solution (Fig.33B). Both the half-wave potential and the current density measured at 0.9V indicate that Pt/DWCNTs exhibit the best activity for ORR (Fig.33B). The half-wave potentials for ORR on Pt/DWCNTs electrode is 0.874V, 10-40 mV more positive as compared with 0.834V for Pt/SWCNTs, 0.864V for Pt/MWCNTs-1 and 0.849V for Pt/MWCNTs-2. The current density for ORR on Pt/DWCNTs is 2.05mA cm^{-2} at 0.9 V, which is also significantly higher than that measured on Pt/SWCNTs (0.88mA cm^{-2}), Pt/MWCNTs-1 (1.72mA cm^{-2}) and Pt/MWCNTs-2(1.30mA cm^{-2}), respectively.

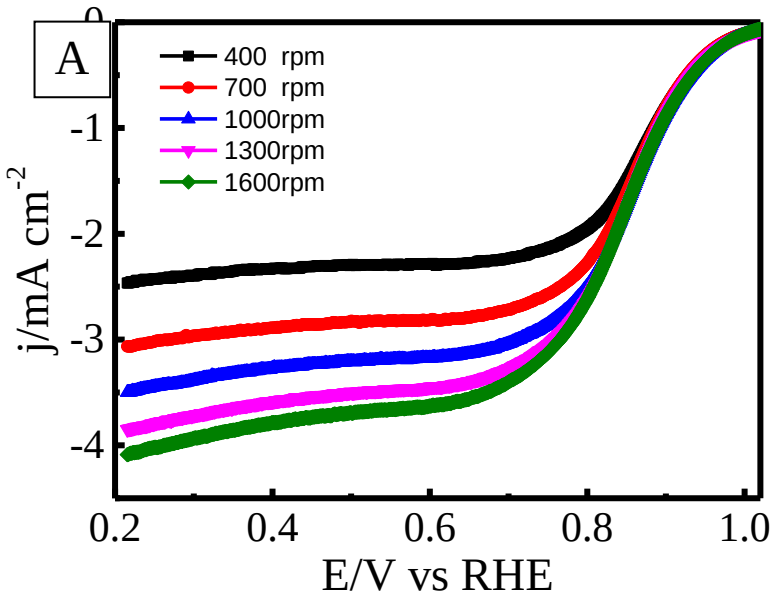

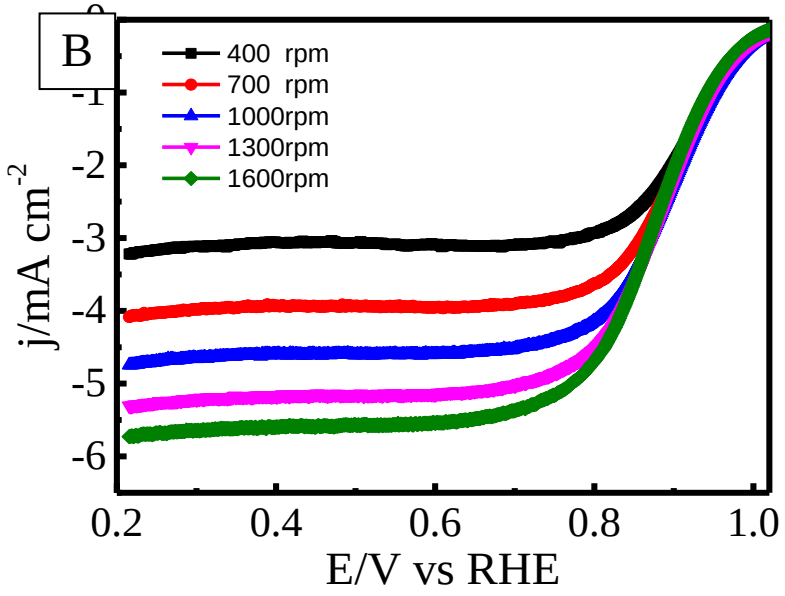
B
400 rpm
700 rpm
1000rpm
1300rpm
1600rpm
j/mA cm-2
-2
-3
-4
-5
-6
0.2
0.4
0.6
0.8
1.0
E/V vs RHE

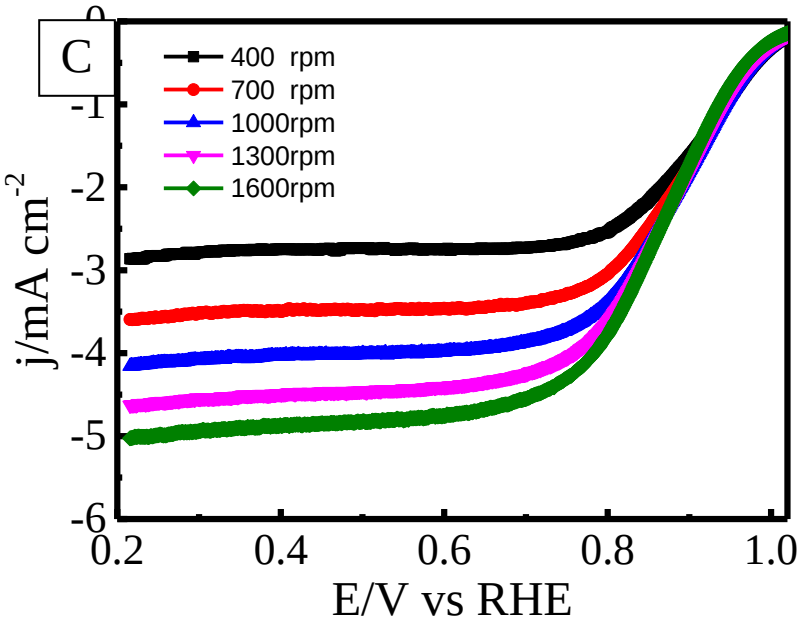
C
400 rpm
700 rpm
1000rpm
1300rpm
1600rpm
j/mA cm-2
-1
-2
-3
-4
-5
-6
0.2
0.4
0.6
0.8
1.0
E/V vs RHE

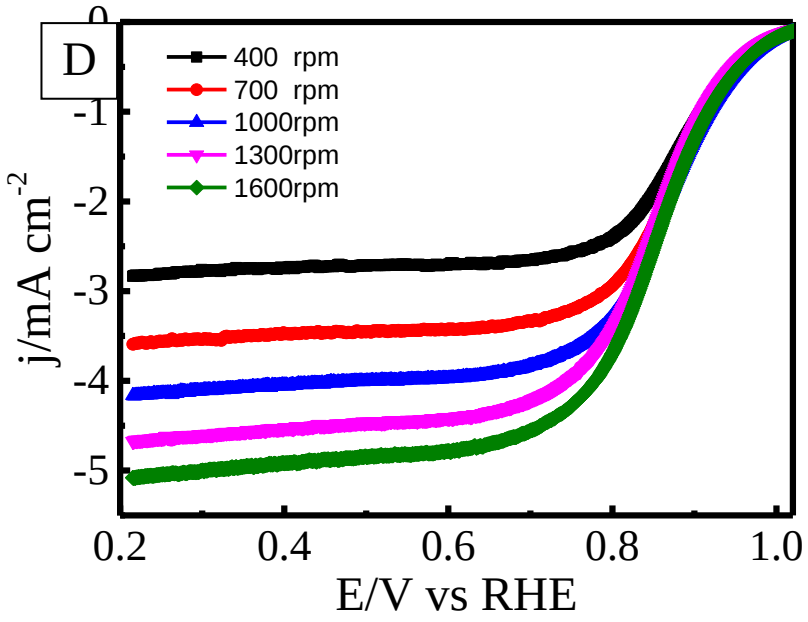
D
400 rpm
700 rpm
1000rpm
1300rpm
1600rpm
j/mA cm-2
0
-1
-2
-3
-4
-5
0.2
0.4
0.6
0.8
1.0
E/V vs RHE

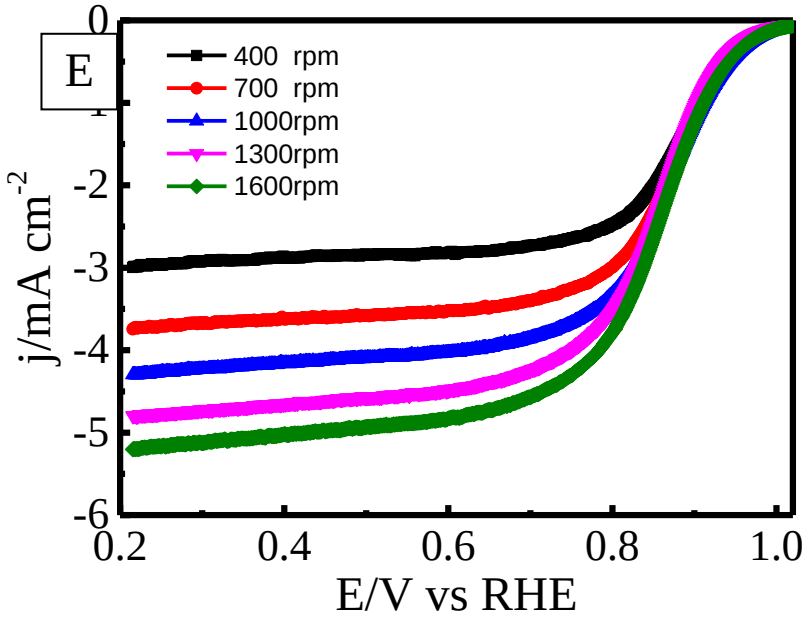
E
400 rpm
700 rpm
1000rpm
1300rpm
1600rpm
j/mA cm-2
0
-2
-3
-4
-5
-6
0.2
0.4
0.6
0.8
1.0
E/V vs RHE

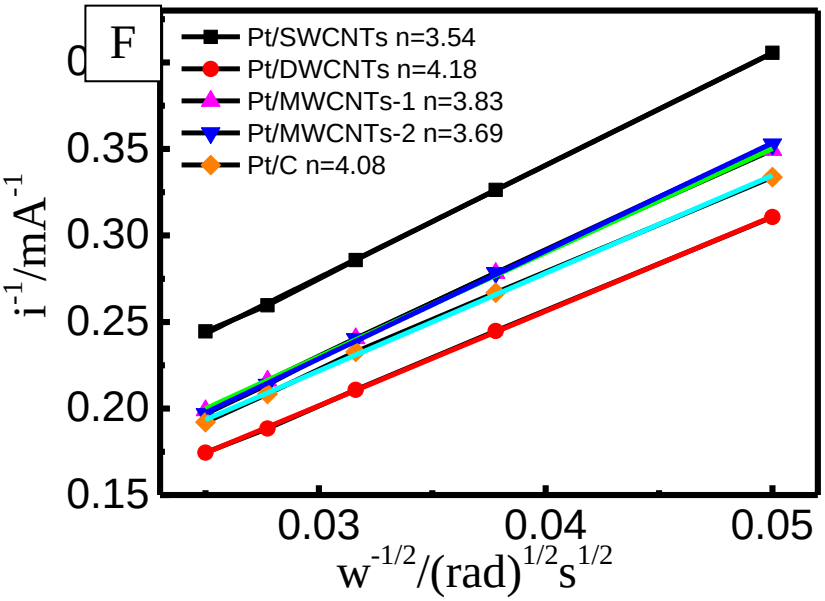

Fig 30Linear scan voltammetry of ORR of four types of Pt/CNTs and Pt/C in at different stirring rate and B) corresponding Koutecky–Levich plots (J^{-1} versus $\omega^{-0.5}$).

The reaction kinetics was studied by rotating-disk voltammetry in order toinvestigate the role of walls during the ORR electrochemical process in alkaline solution. The corresponding Koutecky–Levich plots (J^{-1} vs $\omega^{-1/2}$) at various samples exhibited good linearity (Figure 35 F). Then was calculated to be around 4, with the n of Pt/DWCNTs slightly higher than that of Pt/SWCNTs, Pt/MWCNTs and Pt/MWCNTs-2.

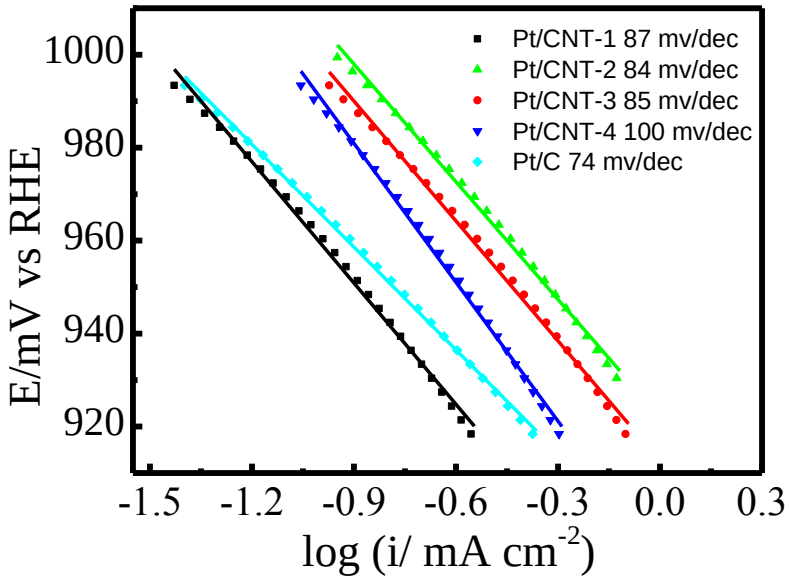

Fig 31 Tafel plots of ORR of Pt/CNTs and Pt/C.

The Tafel plots calculated from the voltammograms are shown in Figure 36. The lowest Tafel slope of -84mV/decade is found for Pt/CNTs-2, which is followed by Pt/CNTs-3 (-85mV/decade), Pt/CNTs-1 (-87mV/decade) and Pt/CNTs-4 (-100mV/decade). This indicates that the rate determining step for the ORR is the first charge transfer step [49-52]:

$O_2 + Pt = Pt(O_2)_{ad}$

It is different from the second rate determining electrochemical step:

$Pt(O_2)_{ad} + e^- = Pt(O_2^-)_{ad.}$

3.4 LSV of Pt/CNTs in acidic solution

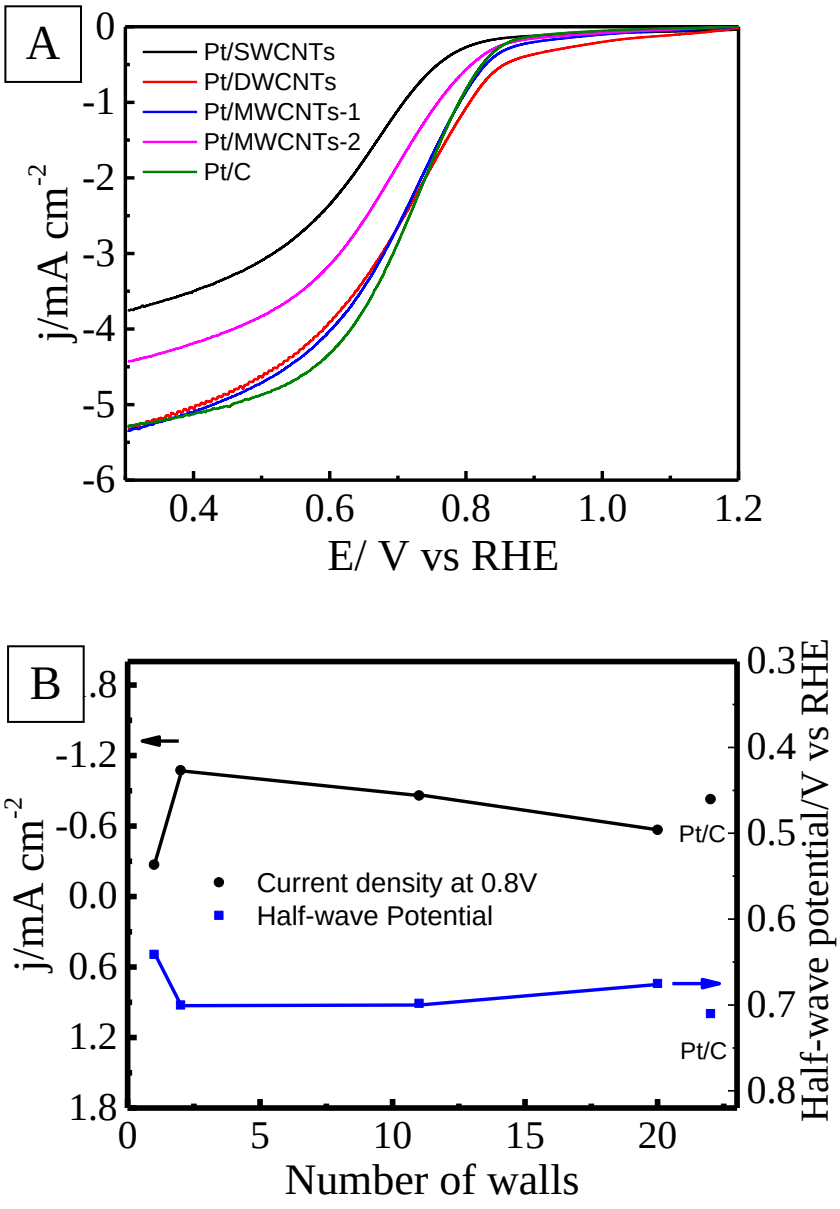

Fig 37A) Linear scan voltammetry of ORRand B) Current density at 0.9 V

Pt/DWCNTs show more excellent activity for ORR, Figure 37 displays the LSV of ORR for Pt/CNTs and summarized the half-wave potential and current density at 0.8 V. The half-wave potential of Pt/DWCNTs is obtained at 0.71 V, about 10-40 mV positive than that observed on Pt/SWCNTs, Pt/MWCNTs-1 and Pt/MWCNTs-2. More importantly, the current density at 0.8 V function as the number of walls exhibits similar volcano shape to that of Pt/CNTs in alkaline solution, indicating the enhanced ORR activity is related with the intrigue properties of CNTs. The ORR current density observed at 0.8 V for Pt/DWCNTs is also 1.07 mA cm^{-2}, significantly higher than that of Pt/SWCNTs, Pt/MWCNTs-1 and Pt/MWCNTs-2 with the number of 0.27, 0.86 and 0.57 mA cm^{-2}, respectively.

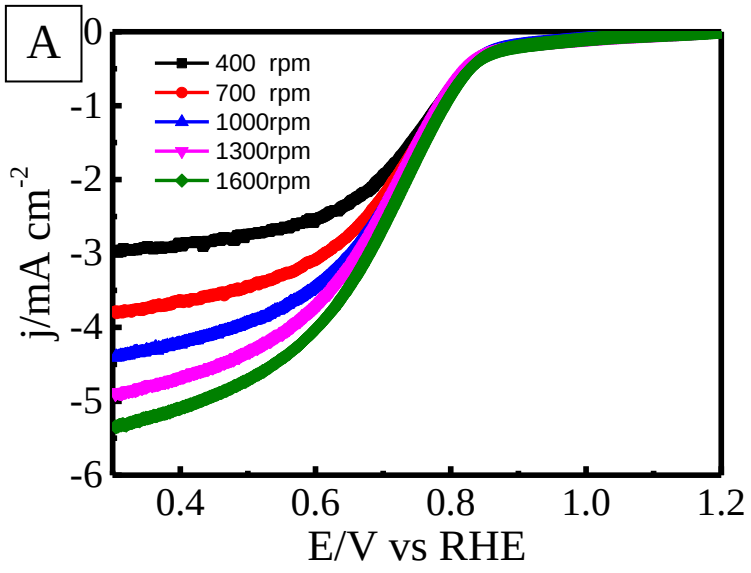

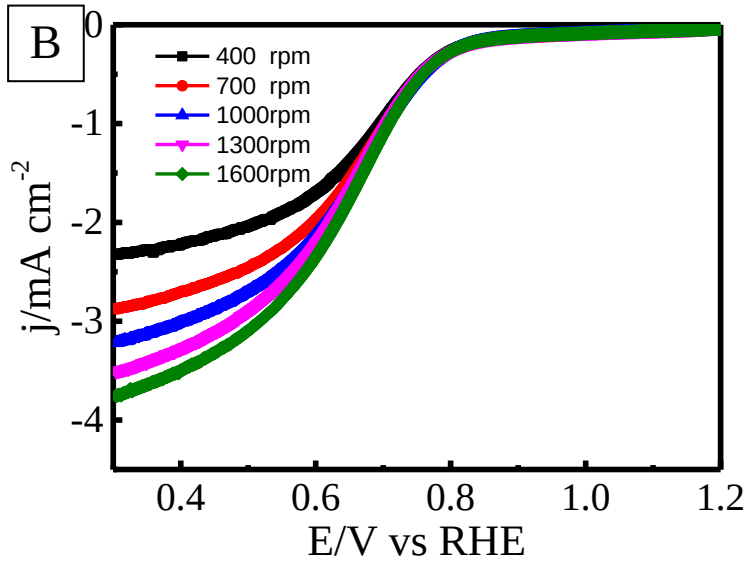

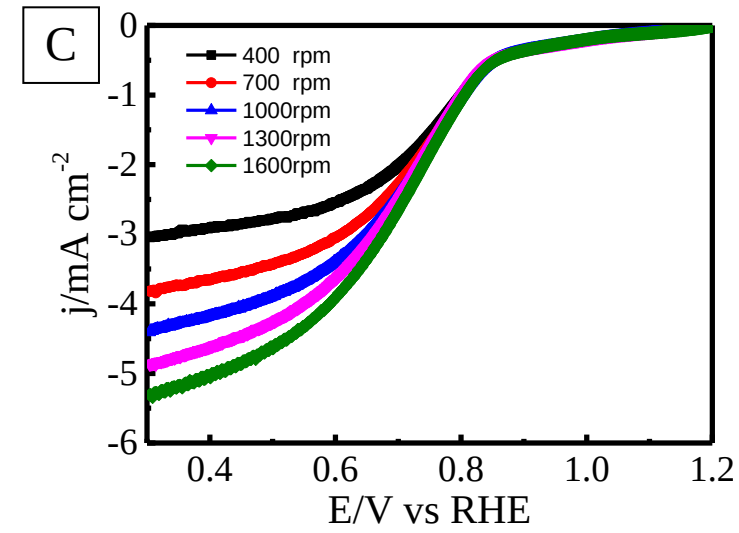
C
400 rpm
700 rpm
1000rpm
1300rpm
1600rpm
j/mA cm-2
E/V vs RHE
0
-1
-2
-3
-4
-5
-6
0.4
0.6
0.8
1.0
1.2

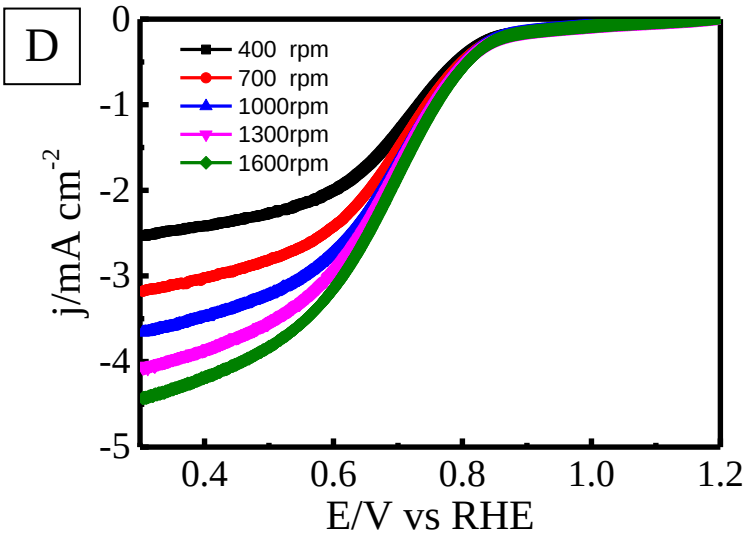
D
400 rpm
700 rpm
1000rpm
1300rpm
1600rpm
j/mA cm-2
E/V vs RHE
0
-1
-2
-3
-4
-5
0.4
0.6
0.8
1.0
1.2

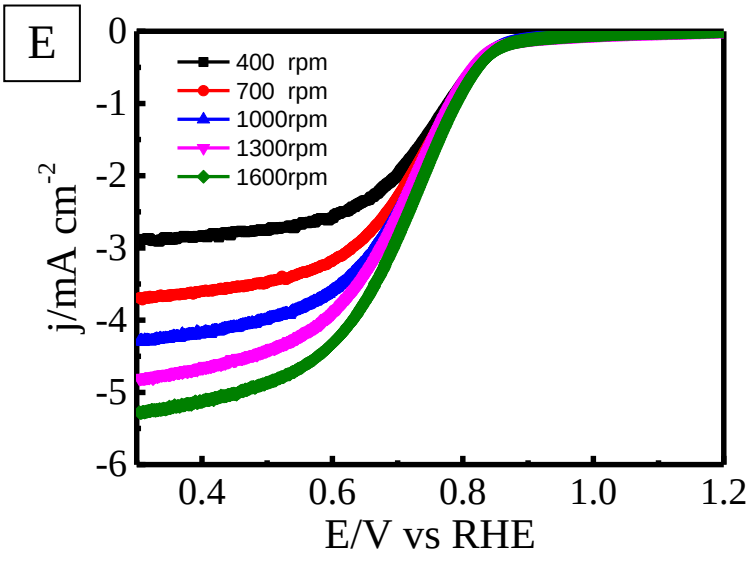
E
400 rpm
700 rpm
1000rpm
1300rpm
1600rpm
j/mA cm-2
E/V vs RHE
0
-1
-2
-3
-4
-5
-6
0.4
0.6
0.8
1.0
1.2

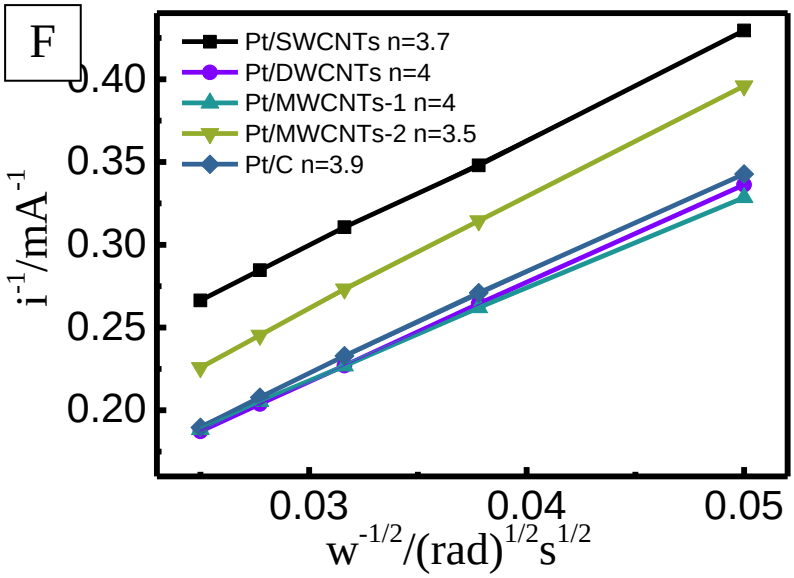

Fig 32Linear scan voltammetry of ORR of four types of Pt/CNTs and B) corresponding Koutecky–Levich plots (J^{-1} versus $\omega^{-0.5}$).

In order to investigate the role of walls during the ORR electrochemical process in acidic solution, the reaction kinetics was studied by rotating-disk voltammetry. The voltammetric profiles in O_2 saturated 0.1 M $HClO_4$ as the electrolyte showed that the current density was enhanced by an increase in the rotation rate (from 400 to 1600 rpm; Figure 37 A-E). The corresponding Koutecky–Levich plots (J^{-1} vs $\omega^{-1/2}$) at various samples exhibited good linearity (Figure 38 F). By using the values $C_0=1.38\times10^{-3}$ mol L^{-1}, $D_0=1.67\times10^{-5}$ cm s^{-1}, and $v=0.1$ m^2 s^{-1} in 0.1 M $HClO_4$, n was calculated to be around 4, with the n of Pt/DWCNTs slightly higher than that of Pt/SWCNTs, Pt/MWCNTs and Pt/MWCNTs-2.

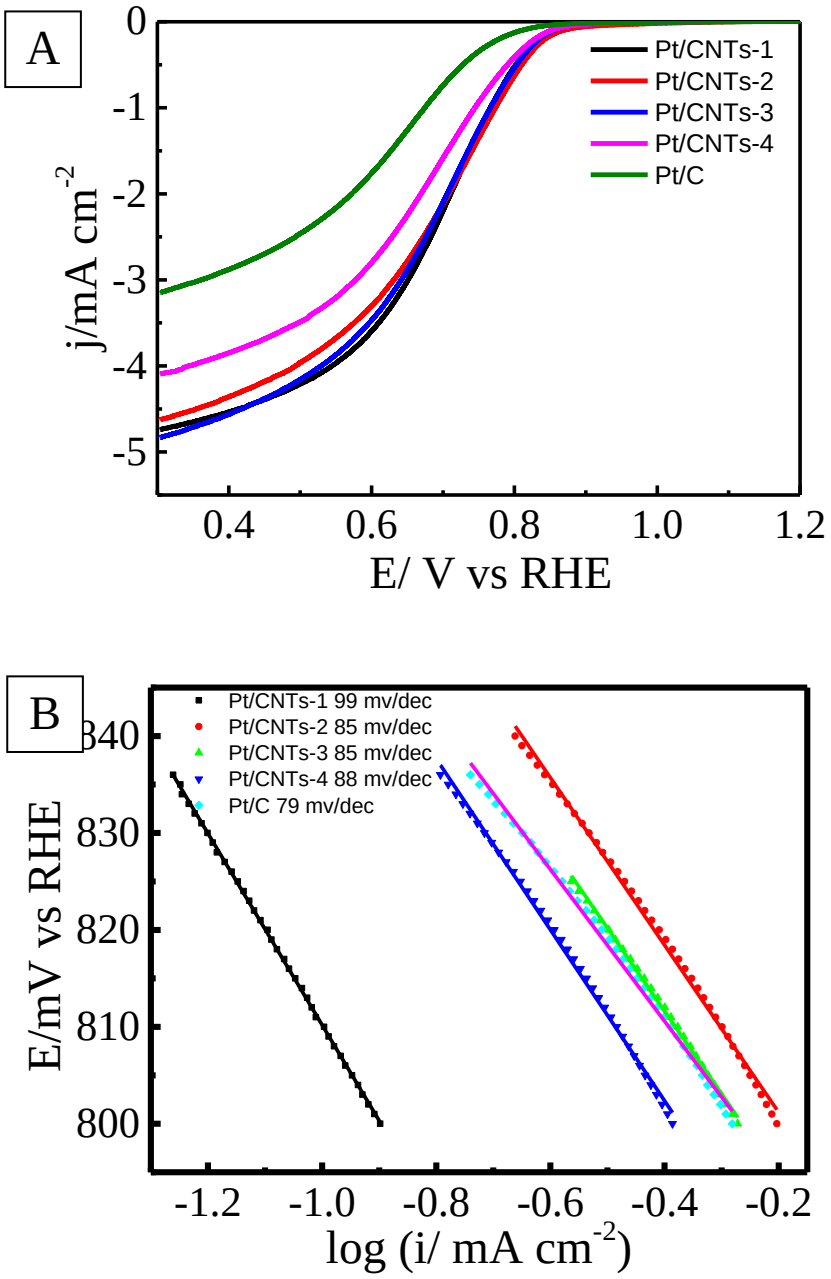

Fig 39(A) Rotating disk voltammograms comparing the oxygen reduction on Pt/CNTs in O_2 saturated 0.1 M $HClO_4$ solution and (B) the corresponding Tafel plots.

The Tafel plots calculated from the voltammograms (Figure 39A) are shown in Figure 39B. A single linear Tafel slope was obtained in the whole potential region.The lowest Tafel slope of -85mV/decade is found for Pt/CNTs-2 and Pt/CNTs-3, which is followed by Pt/CNTs-4 (-88mV/decade) and Pt/CNTs-1 (-99mV/decade). This indicates that the rate determining step for the ORR is the first charge transfer step[49-52]:

$O_2 + Pt = Pt(O_2)_{ad}$

It is different from the second rate determining electrochemical step:

$Pt(O_2)_{ad} + e^- = Pt(O_2^-)_{ad.}$

The ORR activity of Pt/CNTs follows a distinctive volcano-type curves as function to the number of walls of the CNTs, and the best activity are those CNTs composed of DWCNTs supported with Pt NPs. Such distinctive volcano shape is not related with the metal impurities, defects and the surface area of the CNTs as we discussed before. And also is not related with the Pt loading, Pt particle size and ESA due to the loading, the Pt particle size and the ECSA of Pt/CNTs are similar. These evidently indicate that the promotion effect of the CNTs for ORR activity is related to the intrinsic properties of CNTs.

As mentioned before, there is a volcano relationship between the catalytic activity of pristine CNTs and the number of CNTs. DWCNTs with 2-7 walls showbetter performance compared to SWCNTs and large diameter MWCNTs in alkaline solution where 10 mM KCN were applied to eliminate the contribution of the trace amount of metal impurities. Pt and Pd were also supported onto CNTs and the activity for methanol, ethanol and/or formic acid oxidation in alkaline conditions were also investigated, and demonstrated that Pt and Pd NPs supported onto the CNTs with 2-7 inner tubes show significantly better activity for methanol, ethanol and formic acid oxidation compared to those Pt or Pd supported on SWCNTs and MWCNTs. And intriguingly, the activity of Pt/CNTs and Pd/CNTs for methanol and/or ethanol oxidation universally shows a similar volcano-type curve. These results all demonstrated that the electrocatalytic activity of Pt and Pd NPs depends critically on the number of inner tubes of the CNTs supports. The existence of inner tubes with number of 2-7 can facilitate the adsorption and migration of oxygen-containing species and promote the charge transfer between the outer wall and the inner tube via the electron tunnelling effect under electrochemical polarization conditions.

Similar to that of OER, MOR and EOR reaction on CNTs hybrids, the protected inner-tube could also serve as an effective electronic conducting pathway for charge transfer during ORR reaction. Thus the electron tunnelling between the outer wall and the inner tubes could accelerate the electron transfer process during the ORR for pristine CNTs and their hybrids for which is not possible for SWCNTs. As the number of wall increases, the tunnelling resistance will increase significantly due to the tunnelling distance for large diameter MWCNTs (such as CNTs-3 and CNTs-4)

is over 10 Angstroms, which is believed the effective tunnelling distance. Fig. 39 shows the schematic diagram of the promotion effect of CNTs supports. Firstly, the CNTs especially the CNTs compose of 2-5 nm can absorb the O_2 to from H_2O- through a two electron process. And the formed H_2O- can be easily reduced by Pt supported on CNTs. As we discuss before, DWCNTs show better kinetics and enhanced electron transfer properties through tunnelling effect compared with typical SWCNTs and MWCNTs.

4 Conclusions and Future Plans

In conclusion, Pt loaded DWCNTs show significantly better activity for ORR. DWCNTs are demonstrate better catalysts and supports for developing ORR catalysts due to the enhance electron transfer properties of the CNTs composed of 2 inner tubes through tunnelling effect. The present study provides new opportunities to tailor the electro catalytic activity properties of CNTs hybrids via the electron and quantum transport properties of CNTs supports.

The reason for the better performance is due to the quantum effect of double and triple wall carbon nanotubes asshown in Fig. 40. The outer wall is reaction site, while the inner wall is useful for fast electron transfer. As for single wall carbon nanotubes, there is no quantum effect. When it comes to MWCNTs, the effect is decreased with increased wall numbers.

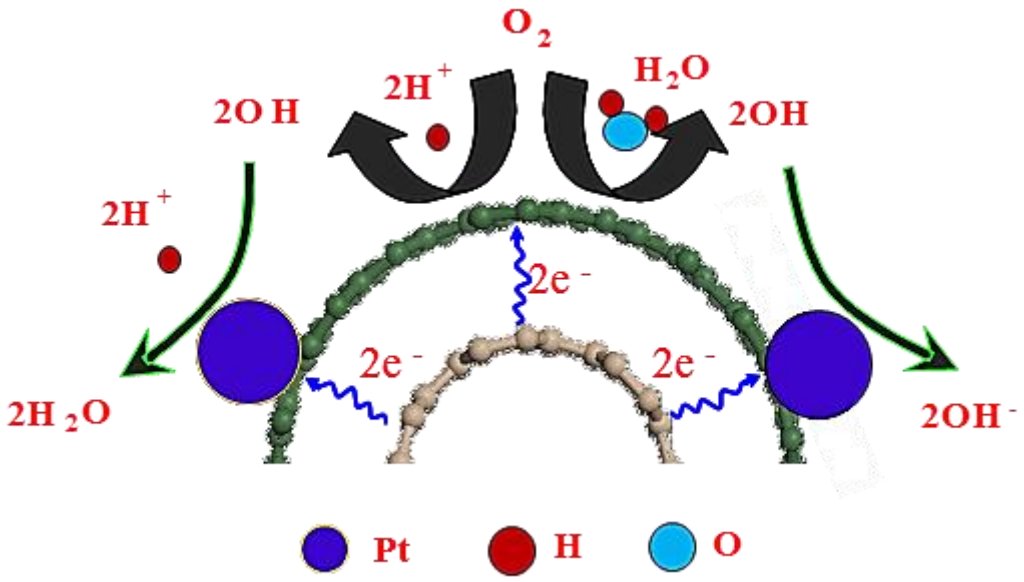

Fig 40 Schematic show of the promotion effect of CNTs for ORR

References

1. Dincer, I., *Renewable energy and sustainable development: a crucial review.* Renewable and Sustainable Energy Reviews, 2000. **4**(2): p. 157-175.
2. Ehsani, M., Y. Gao, and A. Emadi, *Modern electric, hybrid electric, and fuel cell vehicles: fundamentals, theory, and design*. 2009: CRC press.
3. Thomas, C., *Fuel cell and battery electric vehicles compared.* international journal of hydrogen energy, 2009. **34**(15): p. 6005-6020.
4. Song, C. and J. Zhang, *Electrocatalytic Oxygen Reduction Reaction*, in *PEM Fuel Cell Electrocatalysts and Catalyst Layers: Fundamentals and Applications*, J. Zhang, Editor. 2008, Springer London: London. p. 89-134.
5. Srinivasan, S., et al., *Advances in solid polymer electrolyte fuel cell technology with low platinum loading electrodes.* Journal of Power Sources, 1988. **22**(3-4): p. 359-375.
6. Shao, Y., G. Yin, and Y. Gao, *Understanding and approaches for the durability issues of Pt-based catalysts for PEM fuel cell.* Journal of Power Sources, 2007. **171**(2): p. 558-566.
7. Haile, S.M., *Fuel cell materials and components.* Acta Materialia, 2003. **51**(19): p. 5981-6000.
8. Ren, X., et al., *Recent advances in direct methanol fuel cells at Los Alamos National Laboratory.* Journal of Power Sources, 2000. **86**(1): p. 111-116.
9. Gong, K., et al., *Nitrogen-doped carbon nanotube arrays with high electrocatalytic activity for oxygen reduction.* science, 2009. **323**(5915): p. 760-764.
10. Chen, Z., et al., *A review on non-precious metal electrocatalysts for PEM fuel cells.* Energy & Environmental Science, 2011. **4**(9): p. 3167-3192.
11. Othman, R., A.L. Dicks, and Z. Zhu, *Non precious metal catalysts for the PEM fuel cell cathode.* International journal of hydrogen energy, 2012. **37**(1): p. 357-372.
12. Li, S., et al., *Iron-and nitrogen-functionalized graphene as a non-precious metal catalyst for enhanced oxygen reduction in an air-cathode microbial fuel cell.* Journal of Power Sources, 2012. **213**: p. 265-269.
13. Wu, G., et al., *Polyaniline-derived non-precious catalyst for the polymer electrolyte fuel cell cathode.* Ecs Transactions, 2008. **16**(2): p. 159-170.

14. Zhang, J., et al., *Controlling the Catalytic Activity of Platinum‐Monolayer Electrocatalysts for Oxygen Reduction with Different Substrates.* Angewandte Chemie International Edition, 2005. **44**(14): p. 2132-2135.
15. Yeo, K.M., et al., *Surfactant‐Free Platinum‐on‐Gold Nanodendrites with Enhanced Catalytic Performance for Oxygen Reduction.* Angewandte Chemie International Edition, 2011. **50**(3): p. 745-748.
16. Wang, D., et al., *Structurally ordered intermetallic platinum-cobalt core-shell nanoparticles with enhanced activity and stability as oxygen reduction electrocatalysts.* Nature materials, 2013. **12**(1): p. 81.
17. Zhang, J., et al., *Stabilization of platinum oxygen-reduction electrocatalysts using gold clusters.* Science, 2007. **315**(5809): p. 220-222.
18. Alia, S.M., et al., *Platinum-coated palladium nanotubes as oxygen reduction reaction electrocatalysts.* Acs Catalysis, 2012. **2**(5): p. 858-863.
19. Zhu, H., et al., *Synthetic control of FePtM nanorods (M= Cu, Ni) to enhance the oxygen reduction reaction.* Journal of the American Chemical Society, 2013. **135**(19): p. 7130-7133.
20. Iijima, S., *HELICAL MICROTUBULES OF GRAPHITIC CARBON.* Nature, 1991. **354**(6348): p. 56-58.
21. De Volder, M.F.L., et al., *Carbon Nanotubes: Present and Future Commercial Applications.* Science, 2013. **339**(6119): p. 535-539.
22. Eder, D., *Carbon Nanotube-Inorganic Hybrids.* Chemical Reviews, 2010. **110**(3): p. 1348-1385.
23. Wu, J., et al., *Co3O4 nanocrystals on single-walled carbon nanotubes as a highly efficient oxygen-evolving catalyst.* Nano Research, 2012. **5**(8): p. 521-530.
24. Toma, F.M., et al., *Efficient water oxidation at carbon nanotube-polyoxometalate electrocatalytic interfaces.* Nature Chemistry, 2010. **2**(10): p. 826-831.
25. Toma, F.M., et al., *Tailored Functionalization of Carbon Nanotubes for Electrocatalytic Water Splitting and Sustainable Energy Applications.* Chemsuschem, 2011. **4**(10): p. 1447-1451.
26. Ye, W., et al., *Multi-walled carbon nanotube supported Pd and Pt nanoparticles with high solution affinity for effective electrocatalysis.* Applied Surface Science, 2010. **256**(22): p. 6723-6728.
27. Lee, H.-Y., W. Vogel, and P.P.-J. Chu, *Nanostructure and Surface Composition of Pt and Ru Binary Catalysts on Polyaniline-Functionalized Carbon Nanotubes.* Langmuir, 2011. **27**(23): p. 14654-14661.

28. Bambagioni, V., et al., *Pd and Pt–Ru anode electrocatalysts supported on multi-walled carbon nanotubes and their use in passive and active direct alcohol fuel cells with an anion-exchange membrane (alcohol = methanol, ethanol, glycerol).* Journal of Power Sources, 2009. **190**(2): p. 241-251.

29. Hu, C., et al., *Preparation of highly dispersed Pt-SnOx nanoparticles supported on multi-walled carbon nanotubes for methanol oxidation.* Applied Surface Science, 2011. **257**(18): p. 7968-7974.

30. Wang, S., X. Wang, and S.P. Jiang, *PtRu nanoparticles supported on 1-aminopyrene-functionalized multiwalled carbon nanotubes and their electrocatalytic activity for methanol oxidation.* Langmuir, 2008. **24**(18): p. 10505-10512.

31. Wang, D., S. Lu, and S.P. Jiang, *Tetrahydrofuran-functionalized multi-walled carbon nanotubes as effective support for Pt and PtSn electrocatalysts of fuel cells.* Electrochimica Acta, 2010. **55**(8): p. 2964-2971.

32. Liang, Y., et al., *Strongly Coupled Inorganic/Nanocarbon Hybrid Materials for Advanced Electrocatalysis.* Journal of the American Chemical Society, 2013. **135**(6): p. 2013-2036.

33. Chen, Z., et al., *Highly Active Nitrogen-Doped Carbon Nanotubes for Oxygen Reduction Reaction in Fuel Cell Applications.* Journal of Physical Chemistry C, 2009. **113**(49): p. 21008-21013.

34. Yang, L., et al., *Boron-Doped Carbon Nanotubes as Metal-Free Electrocatalysts for the Oxygen Reduction Reaction.* Angewandte Chemie-International Edition, 2011. **50**(31): p. 7132-7135.

35. Shi, Q., et al., *Sulfur and nitrogen co-doped carbon nanotubes for enhancing electrochemical oxygen reduction activity in acidic and alkaline media.* Journal of Materials Chemistry A, 2013. **1**(47): p. 14853-14857.

36. Zhu, J., et al., *One-pot synthesis of a nitrogen and phosphorus-dual-doped carbon nanotube array as a highly effective electrocatalyst for the oxygen reduction reaction.* Journal of Materials Chemistry A, 2014. **2**(37): p. 15448-15453.

37. Miller, T.S., J.V. Macpherson, and P.R. Unwin, *Electrochemical activation of pristine single walled carbon nanotubes: impact on oxygen reduction and other surface sensitive redox processes.* Physical Chemistry Chemical Physics, 2014. **16**(21): p. 9966-9973.

38. Yuan, W., et al., *Significance of wall number on the carbon nanotube support-promoted electrocatalytic activity of Pt NPs towards methanol/formic acid*

oxidation reactions in direct alcohol fuel cells. Journal of Materials Chemistry A, 2015.

39. Zhang, J., et al., *Significant promotion effect of carbon nanotubes on the electrocatalytic activity of supported Pd NPs for ethanol oxidation reaction of fuel cells: the role of inner tubes.* Chemical Communications, 2014. **50**(89): p. 13732-13734.
40. Cheng, Y., et al., *Dye functionalized carbon nanotubes for photoelectrochemical water splitting - role of inner tubes.* Journal of Materials Chemistry A, 2016. **4**(7): p. 2473-2483.
41. Cheng, Y. and S.P. Jiang, *Highly effective and CO-tolerant PtRu electrocatalysts supported on poly(ethyleneimine) functionalized carbon nanotubes for direct methanol fuel cells.* Electrochimica Acta, 2013. **99**(0): p. 124-132.
42. Li, Z., et al., *Novel graphene-like nanosheet supported highly active electrocatalysts with ultralow Pt loadings for oxygen reduction reaction.* Journal of Materials Chemistry A, 2014. **2**(40): p. 16898-16904.
43. Deiner, L.J. *Kinetic Study of the Oxygen Reduction Reaction on Alpha-Ni (OH) 2 and Alpha-Ni (OH) 2 Supported on Graphene Oxide*. in *229th ECS Meeting (May 29-June 2, 2016)*. 2016. Ecs.
44. Wei, J., et al., *Nitrogen‐doped nanoporous carbon/graphene nano‐sandwiches: synthesis and application for efficient oxygen reduction.* Advanced Functional Materials, 2015. **25**(36): p. 5768-5777.
45. Cheng, Y., *Carbon nanotubes based nanostructured catalysts for water electrolysis and fuel cells.* 2014.
46. Cheng, Y., et al., *Pristine carbon nanotubes as non-metal electrocatalysts for oxygen evolution reaction of water splitting.* Applied Catalysis B: Environmental, 2015. **163**: p. 96-104.
47. Wu, H.-X., et al., *In situ growth of copper nanoparticles on multiwalled carbon nanotubes and their application as non-enzymatic glucose sensor materials.* Electrochimica Acta, 2010. **55**(11): p. 3734-3740.
48. Xing, Y., *Synthesis and electrochemical characterization of uniformly-dispersed high loading Pt nanoparticles on sonochemically-treated carbon nanotubes.* The Journal of Physical Chemistry B, 2004. **108**(50): p. 19255-19259.
49. Kongkanand, A., et al., *Single-wall carbon nanotubes supported platinum nanoparticles with improved electrocatalytic activity for oxygen reduction reaction.* Langmuir, 2006. **22**(5): p. 2392-2396.

50. Damjanovic, A. and D. Sepa, *An analysis of the pH dependence of enthalpies and Gibbs energies of activation for O2 reduction at Pt electrodes in acid solutions.* Electrochimica Acta, 1990. **35**(7): p. 1157-1162.

51. Marković, N., et al., *Oxygen reduction reaction on Pt (111): effects of bromide.* Journal of Electroanalytical Chemistry, 1999. **467**(1): p. 157-163.

52. Marković, N., et al., *Structural effects in electrocatalysis: oxygen reduction on platinum low index single-crystal surfaces in perchloric acid solutions.* Journal of Electroanalytical Chemistry, 1994. **377**(1-2): p. 249-259.